University of Reading

Zea mays annexins modulate cytosolic free Ca2+ and generate a Ca2+-permeable conductance

Article

Published Version

Laohavisit, A., Mortimer, J. C., Demidchik, V., Coxon, K. M., Stancombe, M. A., Macpherson, N., Brownlee, C., Hofmann, A., Webb, A. A. R., Miedema, H., Battey, N. H. and Davies, J. M. (2009) Zea mays annexins modulate cytosolic free Ca2+ and generate a Ca2+-permeable conductance. The Plant Cell, 21 (2). pp. 479-493. ISSN 1040-4651 doi: 10.1105/tpc.108.059550 Available at https://centaur.reading.ac.uk/9640/

It is advisable to refer to the publisher's version if you intend to cite from the work. See Guidance on citing.

To link to this article DOI: http://dx.doi.org/10.1105/tpc.108.059550

Publisher: American Society of Plant Biologists

All outputs in CentAUR are protected by Intellectual Property Rights law, including copyright law. Copyright and IPR is retained by the creators or other copyright holders. Terms and conditions for use of this material are defined in the End User Agreement.

University of Reading

www.reading.ac.uk/centaur

CentAUR

Central Archive at the University of Reading

Reading's research outputs online

The Plant Cell, Vol. 21: 479–493, February 2009, www.plantcell.org © 2009 American Society of Plant Biologists

Zea mays Annexins Modulate Cytosolic Free Ca^{2+} and Generate a Ca^{2+}-Permeable Conductance [W]

Anuphon Laohavisit,[a] Jennifer C. Mortimer,[a,1,2] Vadim Demidchik,[a,1,3] Katy M. Coxon,[a,4] Matthew A. Stancombe,[a] Neil Macpherson,[a] Colin Brownlee,[b] Andreas Hofmann,[c] Alex A.R. Webb,[a] Henk Miedema,[d] Nicholas H. Battey,[e] and Julia M. Davies[a,5]

[a] Department of Plant Sciences, University of Cambridge, Cambridge CB2 3EA, United Kingdom
[b] Marine Biological Association, Plymouth PL1 2PB, United Kingdom
[c] Structural Chemistry Program, Eskitis Institute for Cell and Molecular Therapies, Griffith University, Nathan QLD 4111, Australia
[d] BioMaDe, 9747 AG, Groningen, The Netherlands
[e] School of Biological Sciences, University of Reading, Whiteknights, Reading RG6 6AS, United Kingdom

Regulation of reactive oxygen species and cytosolic free calcium ($[Ca^{2+}]_{cyt}$) is central to plant function. Annexins are small proteins capable of Ca^{2+}-dependent membrane binding or membrane insertion. They possess structural motifs that could support both peroxidase activity and calcium transport. Here, a *Zea mays* annexin preparation caused increases in $[Ca^{2+}]_{cyt}$ when added to protoplasts of *Arabidopsis thaliana* roots expressing aequorin. The pharmacological profile was consistent with annexin activation (at the extracellular plasma membrane face) of *Arabidopsis* Ca^{2+}-permeable nonselective cation channels. Secreted annexins could therefore modulate Ca^{2+} influx. As maize annexins occur in the cytosol and plasma membrane, they were incorporated at the intracellular face of lipid bilayers designed to mimic the plasma membrane. Here, they generated an instantaneously activating Ca^{2+}-permeable conductance at mildly acidic pH that was sensitive to verapamil and Gd^{3+} and had a Ca^{2+}-to-K^+ permeability ratio of 0.36. These results suggest that cytosolic annexins create a Ca^{2+} influx pathway directly, particularly during stress responses involving acidosis. A maize annexin preparation also demonstrated in vitro peroxidase activity that appeared independent of heme association. In conclusion, this study has demonstrated that plant annexins create Ca^{2+}-permeable transport pathways, regulate $[Ca^{2+}]_{cyt}$, and may function as peroxidases in vitro.

INTRODUCTION

Annexins form a multigene, multifunctional family of amphipathic proteins with a broad taxonomic distribution covering prokaryotes, fungi, protists, plants, and higher vertebrates (Gerke and Moss, 2002; Morgan et al., 2004, 2006). Found in all plants studied to date and in all organs, these small (32 to 42 kD) proteins can comprise up to 0.1% of total plant cell protein (Delmer and Potikha, 1997; Clark et al., 2001; Moss and Morgan, 2004; Mortimer et al., 2008). The annexin C-terminal core is constructed from four annexin repeats, each comprising five short α-helices. The annexin repeat, of ~70 amino acids, contains the conserved endonexin fold (K-G-X-G-T-{38}-D/E) and is able to bind Ca^{2+} (Kourie and Wood, 2000; Figure 1). Calcium enables the reversible binding of annexins to negatively charged phospholipids, and the Ca^{2+} requirement for binding can be reduced by acidic pH (Blackbourn et al., 1991). In animals, annexins can be cytosolic, membrane associated, or membrane inserted, depending on the prevailing conditions of cytosolic free Ca^{2+} ($[Ca^{2+}]_{cyt}$), pH, and membrane oxidation (reviewed in Gerke and Moss, 2002).

Isolated plant annexins can bind membranes (including secretory vesicles, cell membranes, and endomembranes), GTP/ATP, and F-actin (reviewed in Mortimer et al., 2008). Their roles in planta are poorly understood (Mortimer et al., 2008). Annexins have been found colocalized with anatomical regions of high secretion and growth rates (Blackbourn et al., 1991, 1992; Blackbourn and Battey, 1993; Carroll et al., 1998; Clark et al., 1995, 2001, 2005a, 2005b; Bassani et al., 2004). Maize (*Zea mays*) annexins have been found to stimulate Ca^{2+}-dependent exocytosis in root cap cells (Carroll et al., 1998), the process underlying cell expansion and plant growth (Carroll et al., 1998). Annexin relocation from the cytosol to membranes can occur in response to specific stimuli, such as touch (Thonat et al., 1997), cold (Breton et al., 2000), and salinity (Lee et al., 2004), suggesting a role in adaptive signaling. Indeed, *Arabidopsis thaliana* annexin 1 (*ANN1*) expression is upregulated by peroxide, salicylic acid (Gidrol et al., 1996), abscisic acid (Lee et al., 2004), drought, cold, and salt stress (Cantero et al., 2006). The *ann1*

[1] These authors contributed equally to this work.
[2] Current address: Department of Biochemistry, University of Cambridge, Tennis Court Road, Cambridge CB2 1QW, UK.
[3] Current address: Department of Biological Sciences, University of Essex, Colchester CO4 3SQ, UK.
[4] Current address: Division of Cell Biology, Institute of Ophthalmology, University of London, 11-43 Bath Street, London EC1V 9EL, UK.
[5] Address correspondence to jmd32@cam.ac.uk.
The author responsible for distribution of materials integral to the findings presented in this article in accordance with the policy described in the Instructions for Authors (www.plantcell.org) is: Julia M. Davies (jmd32@cam.ac.uk).
[W] Online version contains Web-only data.
www.plantcell.org/cgi/doi/10.1105/tpc.108.059550

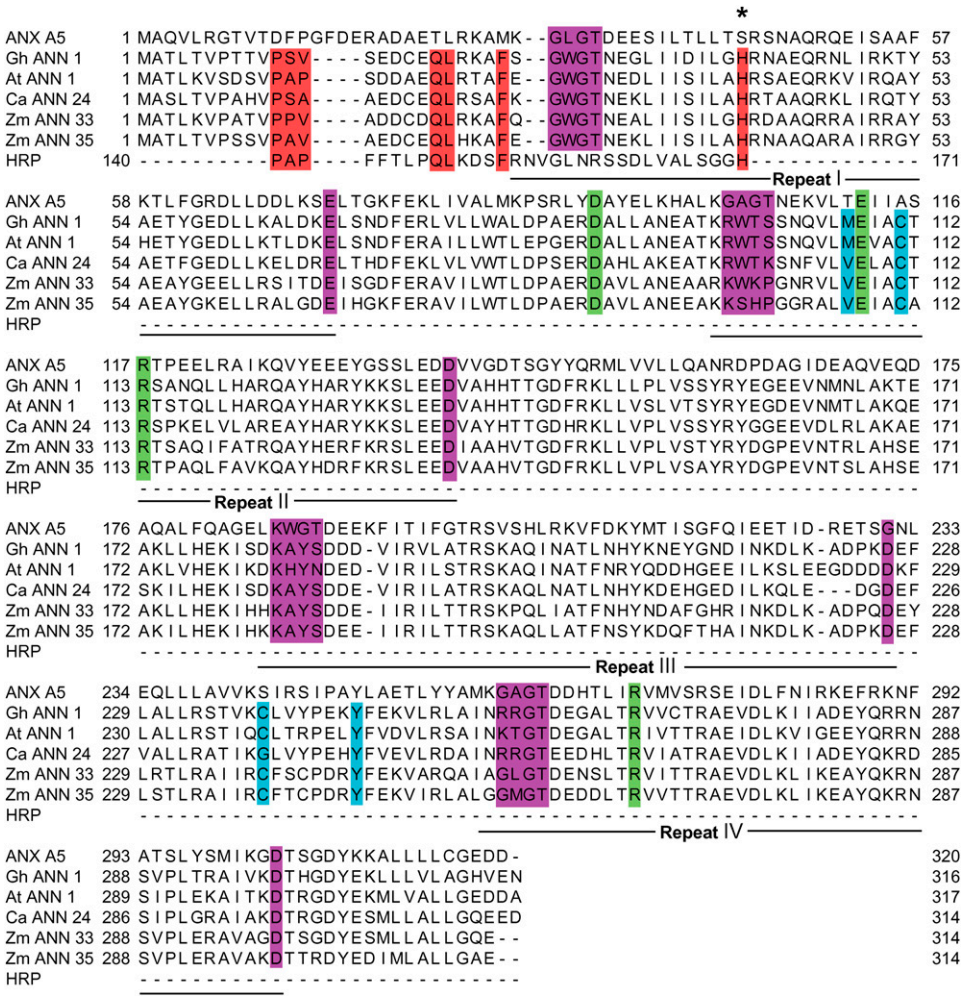

Figure 1. Alignment of Plant Annexin Amino Acid Sequences.

The putative annexin repeats (I to IV) are shown beneath the sequences. The sequences highlighted are as follows: red, comparing the heme binding motif of peroxidase from *Armoracia rusticana* (HRP/140-171) with the N terminus of annexins with identical residues highlighted and the conserved His residue marked (asterisks); blue, the S3 clusters (Hofmann et al., 2003) putatively involved in redox reactions; green, salt bridges involved in channel function of animal annexins (Liemann et al., 1996); purple, endonexin (type II Ca^{2+} binding) sequences; note that only repeats I and IV bind Ca^{2+} ions in plant annexins. The annexin sequences are ANX A5/1-320, Gh ANN 1/1-316, At ANN 1/1-317, Ca ANN 24/1-314, Zm ANN 33/1-314, Zm ANN 35/1-314; accession numbers are given in Methods.

loss-of-function mutant is impaired in osmotolerance (Lee et al., 2004) and primary root growth (Clark et al., 2005b), but the precise roles of ANN1 in these processes remain to be determined.

Results from *Arabidopsis*, *Brassica*, and *Capsicum* point to functions of annexin in ion transport and regulation of cellular activity involving reactive oxygen species (ROS) (Gidrol et al., 1996; Hofmann et al., 2000; Gorecka et al., 2005, 2007; Jami et al., 2008). Initial characterization of recombinant ANN1 has revealed the ability to form K^+-permeable ion channels in planar lipid bilayers (Gorecka et al., 2007) and in vitro peroxidase activity (Gidrol et al., 1996; Gorecka et al., 2005). Recombinant *Brassica juncea* ANN1 also appears to possess peroxidase activity (Jami et al., 2008). *Capsicum annuum* (bell pepper) ANN24 has been found previously to mediate passive Ca^{2+} transport across liposome membranes (Hofmann et al., 2000), consistent with Ca^{2+} channel formation, but effects on $[Ca^{2+}]_{cyt}$ are unknown. Peroxidase activity of plant annexins is thought to be bestowed by a sequence strongly resembling the heme binding region of horseradish peroxidase (Gidrol et al., 1996; Clark et al., 2001; Gorecka et al., 2005). Site-directed mutagenesis of a key His residue (His40) in the putative heme binding region abolished peroxidase activity of recombinant At ANN1 (Gorecka et al., 2005). However, to date there have been no reports of heme binding to annexins from plants nor has the in vivo electron donor been identified. Neither the physiological significance of transport and peroxidase activities nor the extent to which they are shared by other annexins is known. Animal annexins are

variously capable of forming Ca^{2+}-permeable ion channels or modulating the activity of existing channel proteins but lack the heme binding motif (Liemann et al., 1996; Kourie and Wood, 2000). Plant annexins may therefore have more varied cellular functions than their animal counterparts.

Plant cells contain suites of proteins regulating $[Ca^{2+}]_{cyt}$- and ROS-mediated signaling. ROS act in defense and abiotic stress responses (e.g., Zhang et al., 2003; Shin and Schachtman, 2004), control of stomatal aperture (e.g., McAinsh et al., 1996), and growth and development (e.g., Foreman et al., 2003; Liszkay et al., 2004). ROS and $[Ca^{2+}]_{cyt}$ appear to act sequentially in some networks, most notably guard cell abscisic acid signaling (e.g., McAinsh et al., 1996; reviewed in Kwak et al., 2006) and root hair polar growth (Foreman et al., 2003). Thus, a protein such as an annexin with the ability to regulate these two key network components could be a significant control point. Here, to avoid adverse effects of His tags (Hofmann et al., 2000) and ensure correct posttranslational modification, native annexins (ANN33 and ANN35) have been purified from maize to quantify peroxidase activity using an Amplex Red assay.

As maize annexins can potentially form Ca^{2+}-permeable channels or regulate the activity of Ca^{2+} channel proteins, the ability of maize annexins to modulate $[Ca^{2+}]_{cyt}$ has also been addressed. To do this, *Arabidopsis* root epidermal protoplasts have been used as an assay system. These protoplasts have been used extensively in the characterization of native plasma membrane cation or anion channels and $[Ca^{2+}]_{cyt}$ regulation (e.g., Demidchik et al., 2002, 2003; Foreman et al., 2003; Diatloff et al., 2004). As such, they are a useful screening tool for assessing which, if any, channels are annexin regulated. This protoplast assay requires annexin addition to the extracellular plasma membrane face. While ANN33/35 are soluble proteins, they also exist in the maize plasma membrane (Hochholdinger et al., 2005; Carletti et al., 2008) and are predicted to be secreted (SecretomeP program; Bendtsen et al., 2004). Thus, the protoplast assay also tests for annexin interaction with a plasma membrane from the extracellular face. To assess the likelihood of ANN33/35 interaction with the plasma membrane from the intracellular membrane face and test directly for Ca^{2+} transport function, we have incorporated the maize annexins into planar lipid bilayers enriched with the maize plasma membrane phospholipid, phosphatidylethanolamine (see Bohn et al., 2001; Kukavica et al., 2007). The results obtained place plant annexins as potential modulators of both plant cell $[Ca^{2+}]_{cyt}$ and ROS with the ability to generate Ca^{2+}-permeable cation transport pathways.

RESULTS

Maize Annexins Contain a Putative Peroxidase Sequence and Putative Salt Bridges

In silico analysis suggests that plant annexins could be capable of both ion transport function and peroxidase activity. Sequence alignments (Figure 1) reveal that the maize annexins (ANN33 and ANN35) found previously to act as ATP/GTPases (McClung et al., 1994) and stimulate exocytosis (Carroll et al., 1998) contain the putative peroxidase sequence described in At ANN1 (Gidrol et al., 1996; Clark et al., 2001; Gorecka et al., 2005). The ANN1 peroxidase sequence (P-A-P-{5}-Q-L-{3}-F-{17}-H) is identical to that found in horseradish peroxidase (HRP). Overall, ANN33 and ANN35 from maize are 60.6 and 58.7% identical, respectively, to At ANN1 in amino acid sequence, but the putative peroxidase sequence differs from At ANN1 by only two amino acids (P-P-V) in ANN33 and one (P-A-V) in ANN35. ANN33, ANN35, and At ANN1 are 29.3, 28.8, and 31.1% identical, respectively, to human annexin 5 (ANX A5), which exhibits channel activity (Burger et al., 1994; Liemann et al., 1996). The salt bridges (Asp92-Arg117 and Glu112-Arg271) of the hydrophobic pore of ANX A5 (which are involved in ion conduction and selectivity) are perfectly conserved in these plant annexins (Figure 1). Sequence comparison also shows that Ca ANN24 harbors both the peroxidase sequence (differing from At ANN1 by two amino acids; P-S-A) and the two salt bridges (100% identical to ANX A5 despite an overall identity of 32.49%; Figure 1). These data suggest that transport and peroxidase activity could both be exhibited by members of the plant annexin family, spanning monocots and dicots.

An Annexin-Enriched Preparation Induces $[Ca^{2+}]_{cyt}$ Elevation

As sequence analysis revealed the presence of salt bridges indicative of transport capacity in ANN33/35 (Figure 1), we tested for the ability of an annexin-enriched preparation to induce changes in $[Ca^{2+}]_{cyt}$. Calcium-dependent binding to liposomes was used to produce an annexin preparation (see Supplemental Figure 1 online) from maize etiolated coleoptiles as described by Blackbourn et al. (1991) and Carroll et al. (1998). This preparation was found previously to stimulate root cap exocytosis (Carroll et al., 1998). The mean ± SE of total protein yield was 247 ± 139 μg from 40 g of coleoptiles, $n = 3$. In common with the maize annexin preparation used previously by Carroll et al. (1998), two nonannexin proteins (23 and 90 kD) were present in lower abundance (see Supplemental Figure 1 online). These results were reproduced in more than three independent trials, but while the annexins were always the predominant proteins, the relative amounts of the 90-kD contaminant varied with the maize variety used (Mona resulted in greater abundance of the 90-kD band than Earligold).

To test for modulation of $[Ca^{2+}]_{cyt}$ by the annexin-enriched preparation, protoplasts were isolated from fully expanded epidermal cells of *Arabidopsis* roots constitutively expressing (apo) aequorin as a $[Ca^{2+}]_{cyt}$ reporter (Demidchik et al., 2002, 2003; Dodd et al., 2006). With 10 mM $CaCl_2$ in the assay solution, application of the annexin preparation (5 mg/L) to protoplasts caused an initial touch response followed by a transient increase in $[Ca^{2+}]_{cyt}$ lasting ~2 min (Figure 2A). The extracellular Ca^{2+} concentration is not representative of physiological conditions but is used here to help resolve activity. The mean ± SE transient increase in $[Ca^{2+}]_{cyt}$ caused by 5 mg/L annexin preparation was 1.42 ± 0.15 μM ($n = 5$; Figure 2B), and the mean duration was 332 ± 63 s. A lower concentration (2 mg/L) caused a smaller $[Ca^{2+}]_{cyt}$ transient (Figure 2A, middle panel; 0.55 ± 0.70 μM and 239 ± 59 s duration, $n = 4$; $P < 0.01$; Student's t test). Preincubation with 0.1 mM Gd^{3+} as a cation channel blocker completely inhibited

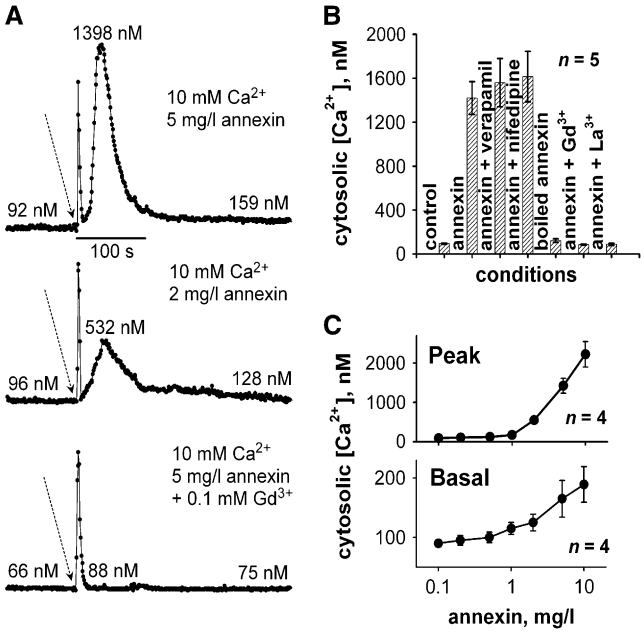

Figure 2. Annexin-Enriched Preparation Elevates $[Ca^{2+}]_{cyt}$ in *Arabidopsis* Root Epidermal Protoplasts.

(A) Increase in $[Ca^{2+}]_{cyt}$. An annexin-enriched preparation added (arrow) to the extracellular membrane face of *Arabidopsis* root epidermal protoplasts (constitutively expressing aequorin) caused a touch-induced transient increase in $[Ca^{2+}]_{cyt}$ followed by a more sustained, dose-dependent increase (top and middle panels). Preincubation with 0.1 mM $GdCl_3$ abolished the response (bottom panel).

(B) Effect of channel blockers on the increase in $[Ca^{2+}]_{cyt}$. Mean ± SE peak transient $[Ca^{2+}]_{cyt}$ responses from 5 mg/L annexin preparation with 10 mM external Ca^{2+}. Channel blockers were incorporated at 0.1 mM ($n = 5$).

(C) Dose dependency of mean ± SE peak transient $[Ca^{2+}]_{cyt}$ response and apparent steady state basal $[Ca^{2+}]_{cyt}$. Basal $[Ca^{2+}]_{cyt}$ was determined 7 to 10 min after the end of the transient ($n = 4$).

the response to the 5 mg/L annexin preparation (Figure 2A, bottom panel). Heat-inactivated annexin preparation was ineffective at elevating $[Ca^{2+}]_{cyt}$ (Figure 2B, $n = 5$). The cation channel blockers verapamil and nifedipine (100 μM) did not inhibit the $[Ca^{2+}]_{cyt}$ increase caused by the annexin preparation (5 mg/L), in contrast with lanthanides (Gd^{3+} and La^{3+}; Figure 2B, $n = 5$). This pharmacological profile matches that of the *Arabidopsis* plasma membrane Ca^{2+}-permeable nonselective cation channels (NSCCs), described previously in this cell type by Demidchik et al. (2002) (i.e., Gd^{3+}-sensitive, verapamil-insensitive). This suggests that the annexin preparation was acting at the extracellular membrane face to modulate the activity of the native NSCC population or was generating a similar Ca^{2+}-conducting pathway.

Examination of dose–response effects revealed that 0.5 mg/L was the lowest concentration of annexin preparation tested capable of causing a statistically significant increase in $[Ca^{2+}]_{cyt}$: Compared with the control (95 ± 6 nM), 0.5 mg/L annexin resulted in a peak $[Ca^{2+}]_{cyt}$ of 120 ± 9 nM, P = 0.065; $n = 4$. The annexin preparation not only caused a dose-dependent transient increase in $[Ca^{2+}]_{cyt}$ but also increased the apparent steady state basal $[Ca^{2+}]_{cyt}$ after the transient (Figures 2A and 2C). The lowest concentration of annexin preparation tested capable of causing a statistically significant increase in basal $[Ca^{2+}]_{cyt}$ was 1 mg/L (control 92 ± 6 nM; 1 mg/L annexin, $[Ca^{2+}]_{cyt}$ 115 ± 10 nM, P = 0.11; $n = 4$). This is consistent with the annexin preparation's stably altering $[Ca^{2+}]_{cyt}$ by acting at the plasma membrane.

Further Purification of Annexins and Identification of Contaminating Proteins

The effects of the annexin preparation on $[Ca^{2+}]_{cyt}$ could be due to, or influenced by, the contaminating proteins. To address this, the ANN33/35 doublet was further purified using size exclusion chromatography. As shown in Figure 3, this removed the 90-kD contaminant. The annexin doublet was apparent after ~5 min of developing the silver stain and remained the only band apparent after 30 min, but overdeveloping (40 min) revealed contamination by the 23-kD protein. To date, we have not been able to separate this protein from the annexin doublet. The 33- and 35-kD bands were confirmed as the maize annexin doublet by matrix-assisted laser-desorption ionization (MALDI) fingerprint. Peptide fragments from the lighter band gave 43% identical coverage to ANN33, and those from the heavier band gave 34% identical coverage to ANN35. The final yield of highly purified ANN33/35 preparation was 33 ± 6 μg (mean ± SE; $n = 5$).

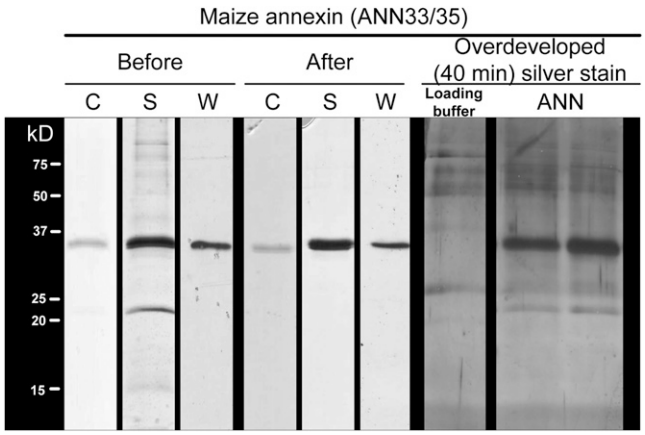

Figure 3. Further Purification of ANN33/35.

Annexins were further purified using lipid binding (before) followed by size exclusion chromatography (after). The gels were either Colloidal Coomassie stained (C), silver stained (S), or used to perform protein gel blot analysis (W) to probe for ANN33/35 using anti-maize annexin antibody (Blackbourn et al., 1991). "Before" and "after" gels were run separately but used protein from the same preparation. The annexin doublet appeared on silver staining for 5 min, and the stains shown were developed for 15 min. Two separate preparations from size exclusion chromatography were used in an overdeveloped silver stain (40 min); samples are shown alongside a control for buffer only. This shows the presence of the p23 contaminant in the highly purified preparation. The sizes of ANN33/35 are 33 and 35 kD, respectively. All lanes were loaded with 3 μg protein.

MALDI fingerprint analysis was also used to explore the identity of the 23- and 90-kD contaminants. The 23-kD protein (p23) is currently absent from maize databases. However, the peptide sequences matched a protein with a mass of ~19 kD (p19) from another plant (resurrection grass [*Sporobolus stapfianus*]; see Supplemental Figure 2 online). *S. stapfianus* p19 is 171 amino acids long and is associated with drought tolerance (Blomstedt et al., 1998; http://www.ncbi.nlm.nih.gov). Gas-phase Edman degradation chemistry was used previously to identify a segment of p23 (Blackbourn et al., 1992). The sequence coverage of the 19-kD protein from *S. stapfianus* became 47% when both results were combined (see Supplemental Figure 2 online). p19 contains a C2 domain (see Supplemental Figure 2 online). This is a Ca^{2+}-dependent domain found in a wide range of proteins implicated in signal transduction and membrane trafficking (for review, see Nalefski and Falke, 1996). Analysis of the maize p23 peptide fragments reveals the presence of part of the consensus C2 domain (DPYV-[X_{12}]-K, where X_{12} signifies 12 amino acids), suggesting that it may be a novel C2 domain protein (see Supplemental Figure 2 online). Analysis of the maize 90-kD band using MALDI fingerprint demonstrated 44% identical coverage of a *Z. mays* lipoxygenase. Plant lipoxygenases (LOX) are non-heme, iron-containing dioxygenases that catalyze the hydroperoxidation of polyunsaturated fatty acids into oxylipins (Porta and Rocha-Sosa, 2002). The sequence of this lipoxygenase from *Z. mays* is 76, 73, and 68% identical to Zm LOX1, Zm LOX2, and Zm LOX4, respectively.

Highly Purified Zm ANN33/35 Preparation Elevates $[Ca^{2+}]_{cyt}$

Root epidermal protoplasts of *Arabidopsis* constitutively expressing apoaequorin were used to investigate the ability of highly purified ANN33/35 preparation to raise $[Ca^{2+}]_{cyt}$. Experimental conditions were the same as those used to test the annexin-enriched preparation (Figure 2). When highly purified ANN33/35 preparation (5 mg/L) was added to protoplasts, a transient increase in $[Ca^{2+}]_{cyt}$ was observed (Figure 4A) that was significantly greater than that caused by buffer alone (ANN33/35 mean ± SE, 0.53 ± 0.05 μM $[Ca^{2+}]_{cyt}$, $n = 3$; buffer control 0.18 ± 0.07 μM $[Ca^{2+}]_{cyt}$, $n = 3$; P = 0.0116, Student's *t* test; Figures 4B and 4F). The elevation of $[Ca^{2+}]_{cyt}$ by 5 mg/L highly purified ANN33/35 preparation was lower than that effected by 5 mg/L of the annexin-enriched preparation (0.53 ± 0.05 μM versus 1.42 ± 0.15 μM, respectively), which may reflect loss of activity incurred during purification or the participation of the contaminant proteins in the tests shown in Figure 2. Similarly, the mean ± SE duration of the transient increase in $[Ca^{2+}]_{cyt}$ induced by highly purified ANN33/35 preparation was shorter than that of the annexin-enriched preparation (5 mg/L: 13 s versus 332 s, respectively). In contrast with the annexin-enriched preparation, highly purified ANN33/35 preparation at 5 mg/L did not significantly increase basal $[Ca^{2+}]_{cyt}$ (i.e., $[Ca^{2+}]_{cyt}$ measured after the transient increase). Mean ± SE resting $[Ca^{2+}]_{cyt}$ prior to ANN33/35 addition was 98 ± 25 nM ($n = 12$), and this returned to 120 ± 33 nM (measured 105 to 150 s after annexin addition, $n = 12$; buffer control, 117 ± 48 nM, $n = 16$). However, in common with the annexin-enriched preparation, elevation of $[Ca^{2+}]_{cyt}$ by highly purified ANN33/35 preparation was sensitive to Gd^{3+} but insensitive to verapamil. Addition of 100 μM verapamil did not block the transient annexin-induced $[Ca^{2+}]_{cyt}$ increase (5 mg/L; 0.57 + 0.03 μM $[Ca^{2+}]_{cyt}$; $n = 4$; Figures 4C and 4F); this was not significantly different to treatment with ANN33/35 alone (P = 0.522). Addition of 300 μM Gd^{3+} prevented $[Ca^{2+}]_{cyt}$ elevation by 5 mg/L highly purified ANN33/35 preparation (0.29 + 0.01 μM, $n = 4$; buffer, 0.26 + 0.02 μM, $n = 4$; P = 0.093, not significantly different; Figures 4D and 4F). To confirm annexin involvement in the $[Ca^{2+}]_{cyt}$ elevation, the highly purified preparation was immunoprecipitated (2:1 antibody: annexin [Carroll et al., 1998]; 10 μg/mL maize antibody: 5 μg/mL maize annexin). As a control, antibody alone or preimmune serum alone was added to the protoplasts. These evoked a small transient, but their peak values were not significantly greater than that caused by buffer alone (antibody alone, 0.29 ± 0.07 μM $[Ca^{2+}]_{cyt}$, $n = 3$; preimmune serum, 0.26 ± 0.02 μM $[Ca^{2+}]_{cyt}$, $n = 3$; buffer control 0.18 ± 0.07 μM $[Ca^{2+}]_{cyt}$, $n = 3$; P = 0.240, Student's *t* test; Figures 4E and 4F). The response evoked by immunoprecipitated annexin preparation was not significantly different from antibody alone (0.29 ± 0.06 μM $[Ca^{2+}]_{cyt}$, $n = 5$; Figures 4E and 4F), thus demonstrating the involvement of annexin in the $[Ca^{2+}]_{cyt}$ response. Overall, the data suggest that highly purified ANN33/35 preparation elevates $[Ca^{2+}]_{cyt}$ in test protoplasts in a manner similar to that of the annexin-enriched preparation. Zm ANN33/35 at the extracellular plasma membrane face most likely activates the native *Arabidopsis* NSCC or generates a similar Ca^{2+}-permeable conductance.

Highly Purified Zm ANN33/35 Preparation Forms a Ca^{2+}- and K^+-Permeable Conductance in Planar Lipid Bilayers

Having used the protoplast $[Ca^{2+}]_{cyt}$ assay as an indicator of maize annexin transport function, the highly purified annexin preparation was incorporated into planar lipid bilayers. This reductionist assay tests for a protein's ability to form an ionic conductance and has been used successfully to address animal annexin transport function (e.g., Burger et al., 1994; Liemann et al., 1996). Phosphatidylethanolamine was used to form bilayers as it is a predominant phospholipid in maize plasma membrane (Bohn et al., 2001; Kukavica et al., 2007) where ANN33 and ANN35 are located (Carletti et al., 2008). Phosphatidylserine was incorporated because annexin binding to phosphatidylserine is a hallmark of this protein family, and cholesterol was used to provide bilayer stability under the ionic conditions used. A mildly acidic pH was chosen to aid annexin incorporation (Langen et al., 1998; Golczak et al., 2001; Gerke and Moss, 2002; Isas et al., 2003; Gorecka et al., 2007). Ca^{2+} and K^+ gradients qualitatively reflected those across the plasma membrane, although absolute levels were higher, as required by the bilayer technique.

Highly purified ANN33/35 preparation (3 μg; the amount used in the silver staining test of purity) was incorporated into planar lipid bilayers of 5:3:2 of 1-palmitoyl 2-oleoyl phosphatidylethanolamine (POPE):cholesterol:1-palmitoyl 2-oleoyl phosphatidylserine (POPS), respectively. In all experiments, the results were from at least three different protein purification preparations. ANN33/35 preparation was added to the *cis*-chamber (cytosolic equivalent), which comprised 1 mM $CaCl_2$, pH 6. The (grounded) *trans*-chamber (extracellular equivalent) comprised

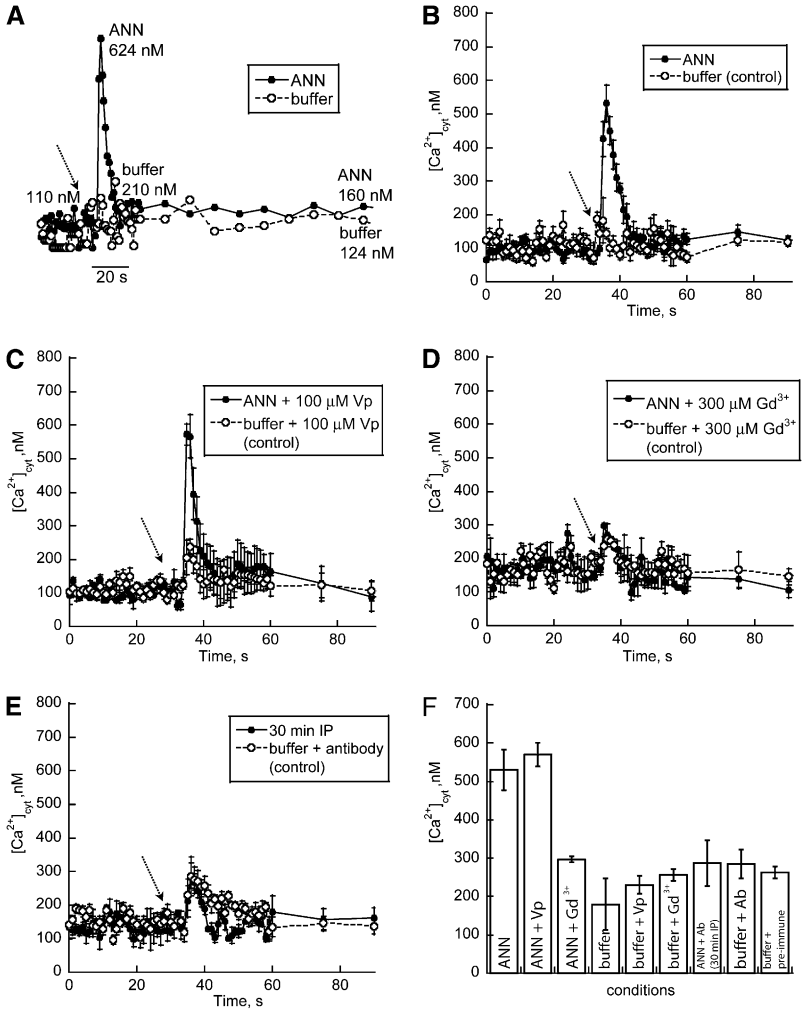

Figure 4. Effect of Highly Purified ANN33/35 Preparation on $[Ca^{2+}]_{cyt}$ of Protoplasts from Mature Root Epidermal Cells.

(A) Example of an annexin-induced increase in $[Ca^{2+}]_{cyt}$. Highly purified maize annexin preparation (5 mg/L) added (arrow; closed circles) to the extracellular membrane face of *Arabidopsis* root epidermal protoplasts (constitutively expressing aequorin) in 10 mM external Ca^{2+} caused a transient increase in $[Ca^{2+}]_{cyt}$. The control experiment adding buffer alone is also shown (open circle).

(B) Mean ± SE $[Ca^{2+}]_{cyt}$ response to 5 mg/L Zm ANN33/35 (closed circle; $n = 3$) or buffer alone (open circle; $n = 4$).

(C) Mean ± SE $[Ca^{2+}]_{cyt}$ response to 5 mg/L Zm ANN33/35 preparation (closed circle; $n = 4$) or buffer alone (open circle; $n = 4$) both in the presence of 100 μM verapamil (Vp).

(D) Mean ± SE $[Ca^{2+}]_{cyt}$ response to 5 mg/L Zm ANN33/35 (closed circle; $n = 4$) or buffer alone (open circle; $n = 4$) both in the presence of 300 μM Gd^{3+}.

(E) Mean ± SE $[Ca^{2+}]_{cyt}$ response to 5 mg/L immunoprecipitated Zm ANN33/35 (IP, closed circle; $n = 3$) or buffer containing equivalent anti-Zm ANN33/35 antibody (open circle; $n = 3$).

(F) Mean ± SE peak $[Ca^{2+}]_{cyt}$ responses from **(B)** to **(E)** and the mean response to preimmune serum at an equivalent concentration to antibody (Ab) used in **(E)** ($n = 3$).

200 mM $CaCl_2$, pH 6.0 (Figure 5A). Under these conditions, a macroscopic conductance was observed in 6 out of 12 attempts in response to a step voltage protocol (Figures 5B and 5C). With a holding membrane voltage of −150 mV, the time taken for the activity to occur was between 40 and 60 min. Macroscopic currents showed no clear time dependency (Figure 5C). As yet, the conditions to support routine resolution of single channel activity have not been elucidated. The mean current-voltage (*I-V*) plot of the macroscopic conductance showed a largely linear relationship between membrane voltage and current (Figure 5D), with the current magnitude similar between inward current (–30 ± 4 pA at –200 mV; $n = 6$) and outward current (29 ± 6 pA at + 200 mV; $n = 6$). Clearly, the annexin preparation would support influx of Ca^{2+} at the hyperpolarized voltages observed for plant plasma membranes. The mean reversal potential (E_{rev}) from the *I-V* relationship in Figure 5D was 9 ± 3 mV ($n = 6$), which is closer to the predicted equilibrium potential for Ca^{2+}, E_{Ca} (+50 mV) than E_{Cl} (–140 mV). The permeability ratio of P_{Ca}/P_{Cl} can be calculated

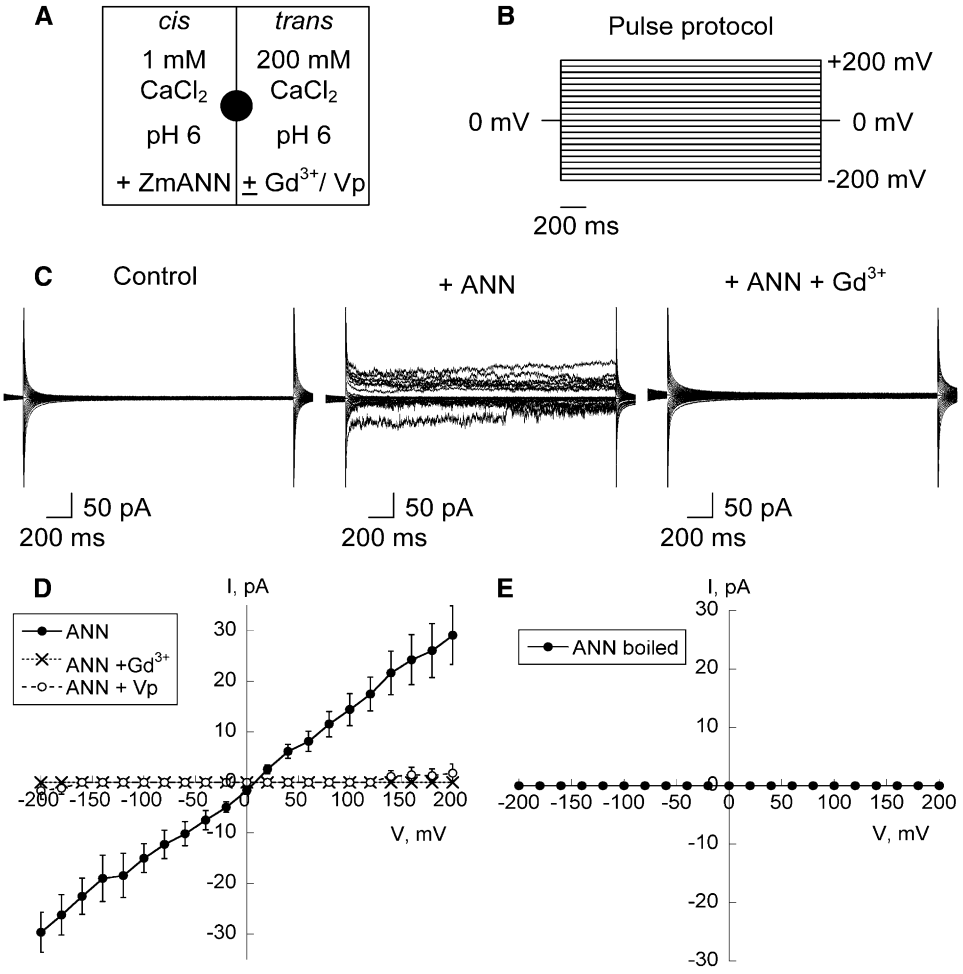

Figure 5. Highly Purified ANN33/35 Preparation Forms a Ca^{2+}-Permeable Conductance in Planar Lipid Bilayers.

(A) Schematic of experimental conditions. Highly purified ANN33/35 preparation (3 μg) was added to the *cis*-chamber, while channel blockers were added to the (grounded) *trans*-chamber. Chambers were separated by a POPE:cholesterol:POPS (5:3:2) bilayer formed across a 200-μm-diameter hole in the septum (filled circle). With this configuration, positive charge flowing from *trans* to *cis* is plotted as negative current, while that flowing from *cis* to *trans* is plotted as positive current.

(B) Schematic of the step voltage pulse protocol used to elicit current.

(C) Representative current traces recorded in response to the voltage protocol applied from a 0 mV baseline. Left panel, prior to annexin addition. Middle panel, current generated by addition of highly purified ANN33/35 preparation. Right panel, effect of 50 μM Gd^{3+} in the *trans*-chamber.

(D) Mean ± SE *I-V* relationships for conditions described in **(A)** and in response to the voltage protocol shown in **(B)**. ANN33/35 (closed circles; $n = 6$), with 50 μM Gd^{3+} (x; $n = 3$) or 50 μM verapamil (open circles; $n = 3$). E_{Ca} was + 50 mV, and E_{Cl} was –140 mV.

(E) Mean ± SE *I-V* relationship for heat-inactivated ANN33/35 ($n = 3$). Conditions as in **(A)** and **(B)**.

from the Goldman equation with the assumption $I_{Ca} + I_{Cl} = 0$ at E_{rev} (Hille, 1992). P_{Ca}/P_{Cl} was calculated to be 5. This conductance was completely blocked by an application of 50 μM Gd^{3+} to the *trans*-compartment ($n = 3$; Figures 5C and 5D) within 5 min after addition. That the blocker was acting at the opposite membrane face to that exposed to the annexin shows that a transbilayer pathway for ions had been formed. The conductance was also substantially blocked by an application of 50 μM verapamil, causing a 94% reduction in mean current amplitude at both –200 mV and +200 mV ($n = 3$; Figure 5D). Heat-inactivated annexin preparation did not evoke a current ($n = 3$; Figure 5E). As the highly purified preparation still contained p23, the preparation was subjected to immunoprecipitation (as described previously) with the anti-ANN33/35 antibody. No currents were evoked over a 3.5 h time frame after adding either antibody alone or immunoprecipitated preparation (3 μg) to the *cis*-chamber ($n = 4$ for each test; see Supplemental Figures 3A to 3C online). This represents a 100% failure rate compared with the 50% observed with normal protein and indicates annexin involvement in current generation. Preimmune serum did not evoke current ($n = 2$). The sensitivity of the highly purified annexin preparation to verapamil in the bilayer assay is in stark contrast with the

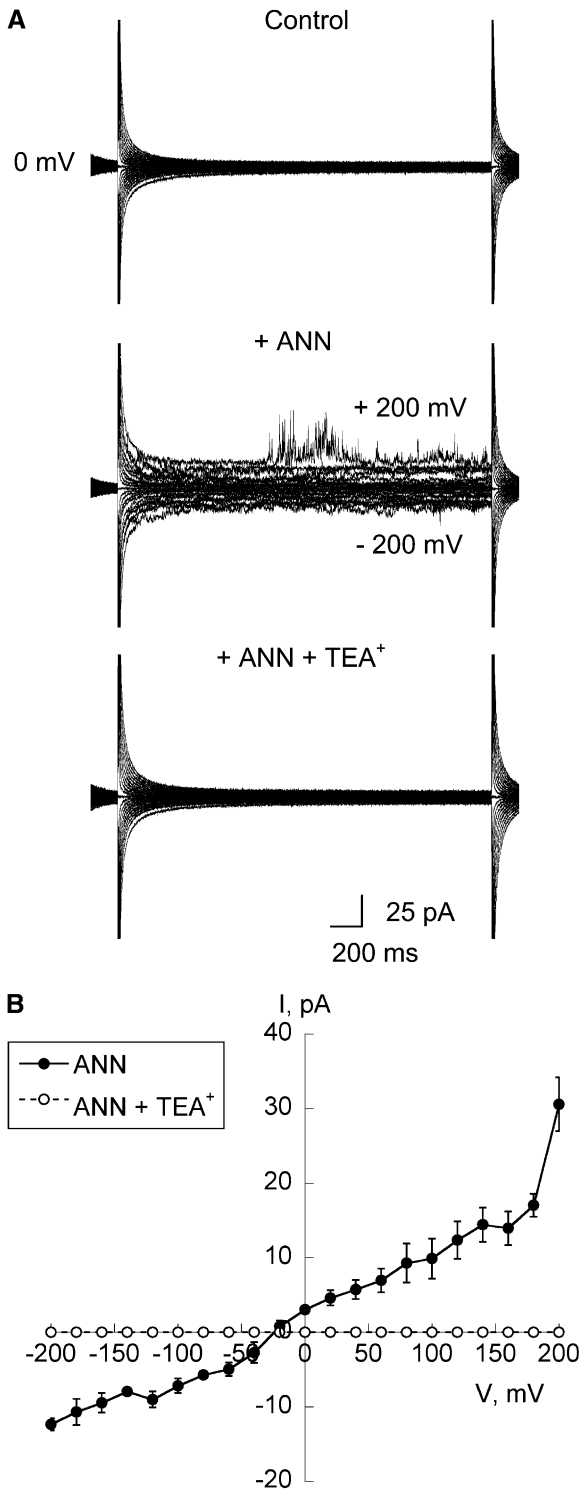

Figure 6. Highly Purified ANN33/35 Preparation Forms a K^+-Permeable Conductance in Planar Lipid Bilayers.

(A) Representative current traces recorded in response to the voltage protocol (as in Figure 5B) applied from a 0 mV baseline. A POPE: cholesterol:POPS (5:3:2) bilayer was used. ANN33/35 preparation (3 μg) was added to the *cis*-chamber comprising 200 mM KCl, pH 6. The *trans*-chamber comprised 50 mM KCl, pH 6.0, ± 50 mM TEA^+. Top panel, prior to annexin addition. Middle panel, current generated by addition of ANN33/35. Bottom panel, effect of 50 mM TEA^+ in the *trans*-chamber.
(B) Mean ± SE *I-V* relationships for ANN33/35 preparation (closed circles; $n = 3$) and effect of 50 mM TEA^+ (open circles; $n = 3$). E_K was of –31 mV, and E_{Cl} was +31 mV.

insensitivity to verapamil of the $[Ca^{2+}]_{cyt}$ response evoked by extracellular annexins in the protoplast luminometry assay (Figures 2 and 4). From this we deduce that the extracellular maize annexins in the latter were activating the verapamil-insensitive native *Arabidopsis* Ca^{2+}-permeable NSCC rather than forming a Ca^{2+}-permeable conductance directly.

The ability of the highly purified ANN33/35 preparation to conduct K^+ (in the absence of Ca^{2+}) was then determined. In all experiments, the results were from at least three different protein purification preparations. With an asymmetrical K^+ gradient (*cis* 200 mM KCl, pH 6; *trans* 50 mM KCl, pH 6), an instantaneously activating macroscopic conductance was observed in three out of five attempts and the time taken for the activity to occur was between 40 and 50 min with a holding membrane voltage of –150 mV (3 μg; Figure 6A). Immunoprecipitated preparation (3 μg) did not evoke a current (3.5 h time frame, $n = 4$; see Supplemental Figure 3D online). The *I-V* generated by the highly purified preparation was essentially linear and current was abolished by application of 50 mM TEA^+, a classic K^+ channel blocker in plants and animals, to the *trans*-chamber ($n = 3$; Figures 6A and 6B). The mean E_{rev} was -27 ± 7 mV ($n = 3$; Figure 6B). This value is closer to the equilibrium potential for K^+ (E_K) of –31 mV than to E_{Cl} (+31 mV) or E_H (0 mV). This shows that K^+ was the predominant ion being transported. The permeability ratio of P_K/P_{Cl} (calculated from the Goldman equation with the assumption that $I_K + I_{Cl} = 0$ at E_{rev}) is 14. Furthermore, P_{Ca}/P_K can be estimated using the P_{Ca}/P_{Cl} value obtained earlier, as the experiments are directly comparable (Véry and Davies, 2000). Thus, a P_{Ca}/P_K value of 0.36 can be obtained (i.e., for every 10 K^+ permeating, 3.6 Ca^{2+} also permeate). This value is typical of plant plasma membrane Ca^{2+}-permeable NSCC (Demidchik et al., 2002, 2003; Demidchik and Maathuis, 2007). As the bilayer experiments mimic transition of ANN33/35 from the maize cytosol to the maize plasma membrane, these data support a model of cytosolic ANN33/35 functioning as a Ca^{2+}-permeable pathway in the native cell.

Maize Annexin Preparations Also Exhibit Peroxidase Activity

Sequence analysis revealed a conserved heme binding peroxidase motif in Zm ANN33/35 (Figure 1), suggesting dual functions in Ca^{2+} transport and ROS regulation. Peroxidase activity of the annexin-enriched preparation was tested using Amplex Red in the presence of H_2O_2. Amplex Red reacts with H_2O_2 with a 1:1 stoichiometry in the presence of a peroxidase to generate the fluorescent oxidation product, resorufin (Zhou et al., 1997). Under standard assay conditions of pH 7.4 and 1 mM H_2O_2, the maize annexin-enriched preparation (25 μg/mL) increased

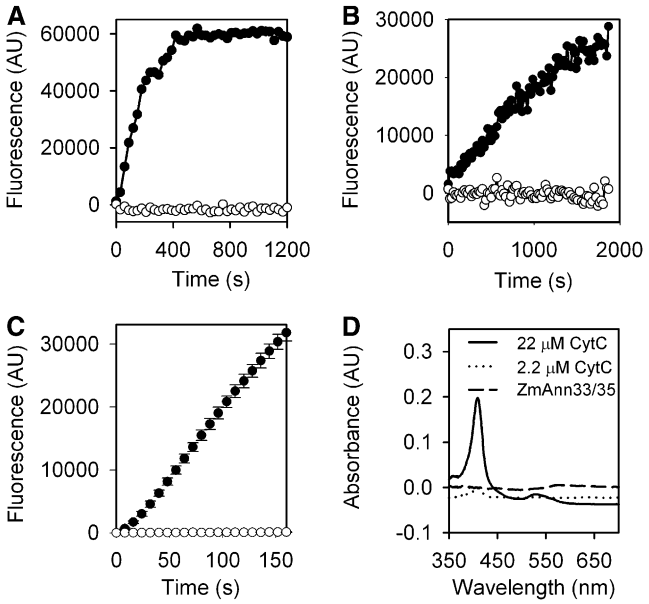

Figure 7. Peroxidase Activity of Maize Annexin Preparations Measured Using Amplex Red.

(A) Time course. Increase in fluorescence (arbitrary units [AU]) supported by 25 μg/mL annexin-enriched preparation at pH 7.4 in the presence of 1 mM H_2O_2 (closed circles) was abolished by heat inactivation (open circles).

(B) Time course of HRP activity (0.095 μg/mL) using conditions described in **(A)**. Heat-inactivated HRP (open circles).

(C) Time course of fluorescence increase supported by 25 μg/mL highly purified ANN33/35 preparation at pH 7.4 in the presence of 1 mM H_2O_2 (closed circles); heat inactivated ANN33/35 preparation (open circles).

(D) Heme detection. Absorption spectrum shows peroxidase-competent annexin-enriched preparation (5 μg) has no Soret peak (~410 nm) indicative of a heme group, in contrast with either 2.2 μM (7.3 ng) or 22 μM (73 ng) cytochrome C oxidase (CytC).

fluorescence, thus demonstrating peroxidase activity, whereas heat-inactivated annexin preparation (boiled for 10 min) did not support an increase (Figure 7A). The mean ± SE rate of fluorescence increase of the annexin-enriched preparation was 38 ± 0.6 $\Delta F\ \mu g^{-1}\ s^{-1}$ ($n = 3$), an order of magnitude lower than that of an HRP positive control (882 ± 28 $\Delta F\ \mu g^{-1}\ s^{-1}$; $n = 3$); no increase in fluorescence was observed with heat-inactivated HRP (Figure 7B). The highly purified ANN33/35 preparation was also tested under standard assay conditions (pH 7.4 and 1 mM H_2O_2). The mean ± SE rate of fluorescence increase generated by the highly purified ANN33/35 preparation at 25 μg/mL (Figure 7C) was 45 ± 2 $\Delta F\ \mu g^{-1}\ s^{-1}$ ($n = 3$), which supports the premise that peroxidase activity of the annexin-enriched preparation was generated by the annexins. Despite the presence of a heme binding motif similar to that of HRP in maize annexins, peroxidase activity appears independent of heme. We tested for the presence of heme using absorbance spectroscopy but were unable to detect the presence of heme in 5-μg protein samples that had supported peroxidase activity (annexin-enriched preparation). By contrast, cytochrome C oxidase as a positive heme control could be diluted to 2.2 μM, an equivalent of 7.3 ng annexin, and still exhibited a Soret absorbance peak (~410 nm) indicative of a heme moiety (Margoliash and Frohwirt, 1959) (Figure 7D).

DISCUSSION

We report that native maize annexins are likely to be multifunctional proteins capable of peroxidase activity, elevation of $[Ca^{2+}]_{cyt}$, and direct formation of a passive Ca^{2+}- and K^+-permeable conductance. It has been estimated that at least 152 proteins in *Arabidopsis* are involved in the regulation of ROS (Mittler et al., 2004). Peroxidases comprise a superfamily of intra- or extracellular heme-containing enzymes catalyzing a number of oxidative reactions, using H_2O_2 as the electron acceptor. Peroxidases are envisaged not only to protect the cell from ROS toxicity but also play a role in signaling, biotic and abiotic stress responses, auxin metabolism, and cell wall modification (reviewed in Passardi et al., 2005). Recombinant *Arabidopsis* ANN1 purified from *Escherichia coli* or *Nicotiana benthamiana* expression systems has peroxidase activity in vitro (Gidrol et al., 1996; Gorecka et al., 2005). A preliminary study found that recombinant Ca ANN24 purified from *E. coli* also has peroxidase activity in vitro (Mortimer, 2007), and recombinant *B. juncea* ANN1 also exhibits peroxidase activity (Jami et al., 2008). Such findings clearly argue for the inclusion of the annexin protein family in considerations of ROS.

Annexin peroxidase activity is reliant on a region of the first annexin repeat (centering on a conserved His residue; His40) that has similarity to the ~30–amino acid heme binding domain of plant peroxidases (Gidrol et al., 1996; Clark et al., 2001; Gorecka et al., 2005). Mutagenesis of His40 in At ANN1 abolished peroxidase activity (Gorecka et al., 2005). Zm ANN33/35 contain the conserved His (Figure 1). Spectral analysis of the annexin-enriched preparation failed to detect heme (Figure 7D). The observation that maize annexin preparations supported peroxidase activity in the apparent absence of an associated heme points to this His residue as being the structural basis for this enzymatic activity in annexins or as being essential for maintaining the overall structure of the annexin molecule. It is possible that annexin peroxidases play a similar role to heme-free glutathione peroxidases (a subgroup of the peroxiredoxins) that catalyze the reduction of lipid peroxides and H_2O_2 to prevent membrane peroxidation and act in (a)biotic stress signal transduction (reviewed in Rouhier and Jacquot, 2005). Peroxidases are distributed throughout roots, and the known ANN33/35 expression in the root elongation zone (Carroll et al., 1998; Bassani et al., 2004) could reflect a role in elongation growth, possibly by limiting H_2O_2 accumulation (Pnueli et al., 2003). This part of the maize root is also the site of ROS accumulation during stress responses, for example aluminum stress (Jones et al., 2006). By extension, loss of peroxidase function could contribute to the short root phenotype of the ANN1 loss-of-function mutant (Clark et al., 2005b; Mortimer, 2007).

Purification of Zm ANN33/35 by lipid binding also resolves 23-kD (p23) and 90-kD (p90) proteins. The association of p23 with lipids is readily explained by the presence of a (partial) C2

domain. The C2 domain mediates Ca^{2+}-dependent phospholipid binding (Nalefski and Falke, 1996). Although few C2-containing proteins have been characterized in plants, the domain has been shown to be essential for plasma membrane association of a mung bean (*Vigna radiata*) phospholipase C (Kim et al., 2004) and a novel bell pepper protein (Kim et al., 2008). To date, plant C2 domain proteins appear to be involved in (a)biotic stress responses and development (Kim et al., 2004, 2008; Yang et al., 2008), suggesting that the novel maize p23 protein could be involved in such Ca^{2+}-dependent processes. The assignment of the p90 as a putative lipoxygenase helps explain its presence in the preparation. Maize lipoxygenases are known to be wound inducible and wound responsive (e.g., Cho et al., 2007). It is possible that the presence of p90 was due to wounding of maize coleoptiles on harvesting. Given that lipoxygenases are compartmentalized on membranes (Porta and Rocha-Sosa, 2002), it is likely that they are obtained during the annexin lipid binding purification process.

Plant annexins have been postulated to act as ion channels (Hofmann et al., 2000). To date, Ca ANN24 has been found to mediate passive Ca^{2+} flux into liposomes by an unknown mechanism (Hofmann et al., 2000), and while At ANN1 has been shown to support K^+ channel activity in planar lipid bilayers, its ability to transport Ca^{2+} is unknown (Gorecka et al., 2007). In common with At ANN1 and Ca ANN24, maize annexins conserve the salt bridges that could confer transport function (Figure 1). Modulation of $[Ca^{2+}]_{cyt}$ by maize annexin preparations demonstrated the capacity to form and/or regulate Ca^{2+} transport pathways in native membranes. Immunoprecipitation experiments demonstrated annexin involvement but cannot preclude the possibility of p23 activity. As highly purified Zm ANN33/35 preparation formed a verapamil-sensitive Ca^{2+}-permeable conductance in bilayers but caused a verapamil-insensitive elevation of $[Ca^{2+}]_{cyt}$ in *Arabidopsis*, the findings point to Zm ANN33/35 regulation of the native *Arabidopsis* plasma membrane verapamil-insensitive NSCC (Demidchik et al., 2002) at the extracellular membrane face to increase $[Ca^{2+}]_{cyt}$.

There are no reports to date of Zm ANN33/35 in the cell wall and so function at the extracellular plasma membrane face in vivo must remain speculative. However, high percentages of plant cell wall proteins appear to be nonclassical secretory proteins and can be predicted using the SecretomeP program (Bendtsen et al., 2004). Maize proteins predicted to be secreted by SecretomeP have now been identified in cell wall fractions (Zhu et al., 2006). ANN33 and ANN35 are predicted to be secreted as are the two predominantly expressed annexins of *Arabidopsis*, ANN1 and ANN2. Although they lack the classic N-terminal signal peptide, both ANN1 and ANN2 have indeed been detected in cell walls (Kwon et al., 2005; Bayer et al., 2006). It is therefore possible that, in some cells, annexins could affect Ca^{2+} transport and $[Ca^{2+}]_{cyt}$ by acting at the extracellular plasma membrane face. There are precedents from animal cells. Animal annexins can be secreted to operate in the extracellular space. In its extracellular form, the channel-forming annexin ANXA5 regulates Polycystin-1 (a transient receptor potential channel) at its extracellular N terminus (Markoff et al., 2007), while extracellular ANXA1 causes $[Ca^{2+}]_{cyt}$ increase by activating plasma membrane G-protein-coupled receptors (Babbin et al., 2006). Generally, the known abundance of annexins in the cytosol and their ability to relocate to plasma and endomembranes (Thonat et al., 1997; Breton et al., 2000; Lee et al., 2004; reviewed in Mortimer et al., 2008) place them predominantly as intracellular regulators of $[Ca^{2+}]_{cyt}$. In this respect, annexins, as regulators of plant channels, can be viewed as being similar to calmodulin. Calmodulin acts at the cytosolic plasma membrane face to regulate cyclic nucleotide-gated channels (Hua et al., 2003) but can also act extracellularly to regulate plasma membrane hyperpolarization-activated Ca^{2+}-permeable channels (Shang et al., 2005).

ANN33/35 are known soluble proteins in maize that also exist in the plasma membrane and possibly tonoplast (Hochholdinger et al., 2005; Carletti et al., 2008). A function at the intracellular plasma membrane face has already been demonstrated by Carroll et al. (1998) who showed an increase in maize root cap plasma membrane capacitance on adding the annexin-enriched preparation to protoplast cytosol. Here, the bilayer experiments mimicked movement of ANN33/35 from the cytosol to the plasma membrane and showed the ability of ANN33/35 to generate a Ca^{2+} influx pathway at slightly acidic pH (pH 6). This agrees with animal studies in which acidic pH promotes channel activity (Langen et al., 1998; Golczak et al., 2001; Isas et al., 2003) and the ability of At ANN1 to from a K^+-permeable conductance at pH 5.8 (Gorecka et al., 2007). Immunoprecipitation experiments confirmed annexin involvement in conductance formation but, strictly, the possibility remains that the conductance was formed by the low level p23 contaminant with the aid of the annexins or that both p23 and annexins were required. A macroscopic conductance was observed more frequently than single channel events, and this has also been reported for animal annexins (Arispe et al., 1996). Blockage by Gd^{3+} is also consistent with the pharmacology of animal annexin channels (Kourie and Wood, 2000), but Ca^{2+} permeability is low compared with animal counterparts (P_{Ca}/P_K 0.36 versus 4.34 for single channel ANXA5; Burger et al., 1994; Liemann et al., 1996). Site-directed mutagenesis of ANXA5 salt bridges dramatically decreases Ca^{2+} permeability to 0.87 (Burger et al., 1994), suggesting that subtle sequence differences in plant annexins could cause low Ca^{2+} permeability. This possibility and the mode of conductance formation by plant annexins now need to be determined.

The channel proteins of the maize plasma membrane are increasingly well understood at the molecular level. Inward and outward K^+-selective rectifiers are known to be encoded by members of the *Shaker* family (Philippar et al., 2003; Büschenschütz et al., 2005; Su et al., 2005). The genetic identities of the less selective and instantaneously activating channels remain unknown. The K^+-permeable, instantaneously activating conductance formed by the ANN33/35 preparation resembles the maize MgC conductance that has been characterized by patch clamp electrophysiology in guard and subsidiary cell plasma membranes (Wolf et al., 2005). However, unlike MgC, the ANN33/35 conductance is sensitive to block by TEA^+. The sensitivity of the ANN33/35 conductance to verapamil also distinguishes this conductance from those characterized in maize plasma membrane vesicles by $^{45}Ca^{2+}$ flux analysis (Marshall et al., 1994). It may be that ANN33/35 ($\pm$ p23) underpins the instantaneous and TEA^+-sensitive K^+-permeable conductance observed in root and suspension cell plasma membranes (Ketchum et al.,

1989; Roberts, 1998). Analysis of loss-of-function mutants is now needed to resolve in planta transport function, which at the plasma membrane could support Ca^{2+} influx for signaling and K^+ flux for voltage regulation.

Annexin expression is dynamic and responsive to stress conditions known to increase $[Ca^{2+}]_{cyt}$ and ROS, such as salinity, cold, and nutrient deprivation (reviewed in Mortimer et al., 2008). Such conditions cause relocation of annexins from the cytosol to membranes, sometimes also causing annexin insertion into membranes (Breton et al., 2000; Lee et al., 2004). The findings here (that annexins can act as peroxidases, modulate $[Ca^{2+}]_{cyt}$, and form a Ca^{2+}-permeable K^+ conductance) firmly place the dynamic behavior of annexins in a signaling context. ANN33/35 are expressed in roots, coleoptiles, and egg cells (Blackbourn et al., 1991; Carroll et al., 1998; Bassani et al., 2004: Okamoto et al., 2004; Hochholdinger et al., 2005; Carletti et al., 2008) where $[Ca^{2+}]_{cyt}$ and ROS regulation will be pivotal to development and adaptation. The amount of ANN33/35 in root plasma membrane is now known to increase in response to environmental conditions (Carletti et al., 2008), consistent with a signaling role. Additionally, that acidic pH supports a Ca^{2+}-permeable conductance by ANN33/35 ($\pm$p23) suggests that it could function in Ca^{2+} signaling in response to stress-induced cytosolic acidosis. For example, anoxia causes root tip cytosolic acidosis in maize, and while the Ca^{2+} signal for metabolic adaptation appears to emanate from mitochondria, the Ca^{2+} signal for an adaptive localized cell death comes from the plasma membrane (Chang et al., 2000; Subbaiah et al., 2000).

The molecular identities of higher plant Ca^{2+}-permeable channels are now being established. The impact of loss of function on $[Ca^{2+}]_{cyt}$ is used to associate Ca^{2+} transport with a gene, while heterologous expression can permit Ca^{2+} permeation of the gene product to be ascertained, provided that expression does not affect native conductances. Combining these approaches has confidently identified TPC1 (Two Pore Channel 1) and CNGC2 (Cyclic Nucleotide-Gated Channel 2) as Ca^{2+}-permeable channels in *Arabidopsis* (Leng et al., 2002; Peiter et al., 2005; Ali et al., 2007). Other CNGCs and members of the glutamate receptor family are strong candidates as potential Ca^{2+}-permeable channels (Meyerhoff et al., 2005; Urquhart et al., 2007; Tapken and Hollmann, 2008), while the *Arabidopsis* Stelar K^+ Outward Rectifier has also been found to be Ca^{2+} permeable (Gaymard et al., 1998). Bilayers provide unequivoval evidence for Ca^{2+} transport by a single protein. The determination here of Ca^{2+} transport by maize annexins in bilayers clearly adds this family of proteins to the suite of higher plant Ca^{2+} transporters. With eight annexins in *Arabidopsis* (Cantero et al., 2006) and nine in rice (*Oryza sativa*; Moss and Morgan, 2004) to explore, these enigmatic, multifunctional proteins now need to be considered in the networks translating cellular signals.

METHODS

Plant Growth

Seeds of maize (*Zea mays* cv Mona [Pioneer Hi-Bred International] or Earligold [Moles Seeds]) were soaked overnight in aerated distilled water. Seeds were grown in the dark on damp vermiculite in propagators for 6 to 9 d at room temperature. *Arabidopsis thaliana* [Columbia-0 wild type and constitutively expressing cytosolic (apo)aequorin, driven by the cauliflower mosaic virus 35S promoter] was grown aseptically at 22°C for 10 to 15 d (16-h daylength; 100 μmol/m^2/s irradiance) on full-strength Murashige-Skoog medium (Duchefa) with 1% (w/v) sucrose and 0.3% (w/v) Phytagel (Sigma-Aldrich).

Annexin Production

Maize etiolated coleoptiles (40 g) were ground with liquid nitrogen in a mortar and pestle to a fine powder. The purification protocol was based on Blackbourn et al. (1991). Homogenization buffer (0.15 M NaCl, 10 mM HEPES, 10 mM EDTA, and 1 mM PMSF, pH 7.4) was added and the mixture filtered through two layers of muslin. After centrifugation (30 min) to remove remaining debris (30,000*g*), the supernatant was added to liposomes. These were prepared from bovine brain lipid (Folch fraction IV; Sigma-Aldrich) dissolved in chloroform:methanol (2:1; 15 mg/mL) and then formed by the addition of liposome buffer (50 mM HEPES, 150 mM NaCl, 5 mM EGTA, and 1 mM PMSF, pH 7.5) and brief vortexing. Alternatively, liposomes were prepared from soybean asolectin (200 mg; Fluka) dissolved in (2:1) chloroform:methanol to give a final concentration of 13.3 mg/mL. $CaCl_2$ was added to liposomes to a final concentration of 10 mM, and the suspension was incubated on ice for 1 h, followed by centrifugation for 30 min (30,000*g*). The supernatant was discarded and the pellet was resuspended in wash buffer (0.15 M NaCl, 10 mM HEPES, 10 mM $CaCl_2$, and 1 mM PMSF, pH 7.4). Following centrifugation for 30 min (30,000*g*), the pellet was resuspended in wash buffer lacking NaCl. The centrifugation step was repeated, and the pellet was resuspended in elution buffer (0.15 M NaCl, 10 mM HEPES, 15 mM EDTA, and 1 mM PMSF, pH 7.4). After a final centrifugation step (1 h, 100,000*g*), the supernatant was collected and added to bovine brain or asolectin liposomes; the entire process was then repeated. After the final centrifugation, the buffer was exchanged to 10 mM K-PO_4 buffer, pH 7.4, and the sample concentrated using a centricon (molecular weight cutoff 10 kD; Amicon). All steps were performed at 4°C. The concentrated sample was then loaded onto a gel filtration column (Superose 12; Amersham) attached to an FPLC system. The column was equilibrated with 10 mM K-PO_4 buffer, pH 7.4. Maize annexins (ANN33/35) were eluted with this buffer at a flow rate of 0.4 mL/min. Fractions of 1 mL were collected and tested for ANN33/35 by SDS-PAGE and protein gel blot analysis. All proteins were exchanged into buffer (10 mM K-PO_4 buffer, pH 7.4) prior to use. In immunoprecipitation studies, the maize annexin preparation was incubated for 30 min at room temperature with anti-ANN33/35 antibody (Blackbourn et al., 1991) in a 2:1 ratio (Carroll et al., 1998). Antibody or preimmune serum alone was added as a control. Protein concentration was estimated using Protein Assay Reagent (Bio-Rad) calibrated against BSA (Sigma-Aldrich).

Gel Electrophoresis and Immunoblotting

Samples were incubated for 10 min at 90°C in buffer (10% [w/v] sucrose, 5% [v/v] β-mercaptoethanol, 2% [w/v] SDS, 0.001% [w/v] bromophenol blue, and 50 mM Tris-HCl, pH 6.8). Samples were first run through a 4% (w/v) acrylamide stacking gel at 70 V and then through a 12% (w/v) acrylamide resolving gel at 150 V for 70 min. Gels were either immunoblotted or stained using either Colloidal Coomassie Brilliant Blue (Sigma-Aldrich) or Silver Stain Plus (Bio-Rad). For silver staining, gels were fixed overnight to enhance detection and then washed twice for 20 min with distilled water to ensure that all acetic acid in the gel during the fixative step was washed away to prevent its slowing down band resolution on staining. Staining was conducted for up to 40 min. For immunoblotting, proteins were electroblotted onto polyvinylidene fluoride (GE Healthcare) using transfer buffer (25 mM Tris, 200 mM glycine, and 20% [v/v] methanol) at 4°C, 60 V, for 3 h. Membranes were blocked by incubating

overnight at 4°C in TBS-T (20 mM Tris, 150 mM NaCl, and 0.1% [w/v] Tween 20, pH 7.6) containing 5% (w/v) skimmed milk powder (Sainsburys). Following washing in TBS-T, membranes were incubated with primary antibody (1:5000 dilution of the anti-ANN33/35 antibody described in Blackbourn et al., 1991) for 1 h, at room temperature, with shaking then after washing for a further 1 h with secondary antibody (1:5000 peroxidase-linked anti-rabbit IgG; Invitrogen). Proteins were visualized using enhanced chemiluminesence (ECL-plus; GE Healthcare) according to the manufacturer's instructions.

Protein Verification

Protein identity was determined by mass spectrometry. Samples were subjected to SDS-PAGE with slight modification. All solutions for SDS-PAGE were membrane filtered. Gels were stained with Coomassie Brilliant Blue or Colloidal Coomassie blue (Sigma-Aldrich) and destained in filter-sterilized 10% (v/v) methanol once. The gel was stored in 10% (v/v) methanol prior to in-gel digestion and MALDI peptide mass fingerprint analysis (Protein and Nucleic Acid Chemistry Facility; University of Cambridge). Protein identifications were based on multiple peptide matches.

$[Ca^{2+}]_{cyt}$ Determination

Protoplasts were isolated from fully expanded root epidermal cells as described by Demidchik et al. (2002) and suspended in holding solution (HS) comprising 5 mM KCl, 2 mM $CaCl_2$, 1 mM $MgCl_2$, 10 mM sucrose, 10 mM glucose, and 2 mM MES, pH 5.7, with Tris (290-300 mOsM). Protoplasts were incubated in HS with 4 μg/mL coelentrazine (free base; NanoLight Technology) for 3 h in the dark (28°C) and then washed in recording solution (10 mM $CaCl_2$ unless stated otherwise; osmotic potential and pH were as in HS, colentrazine was maintained at 4 μg/mL) before being placed in luminometer cuvettes. Annexin preparation was added at 0.1 to 10 mg/L; heat-inactivated annexin was used as a control. Channel blockers (Sigma-Aldrich) were incorporated into the assay prior to annexin addition. Luminometry and calibration to convert luminescent values to $[Ca^{2+}]_{cyt}$ were performed as described by Dodd et al. (2006).

Planar Lipid Bilayers

Lipids were obtained from Avanti Polar Lipids or Sigma-Aldrich. These were POPE, POPS, and cholesterol. Lipids (25 mg/mL) were mixed in the proportions required. Bilayers were composed of POPE:cholesterol:POPS (5:3:2). Lipid dispersions (10 mg/mL) were prepared by evaporating the chloroform under a stream of nitrogen and resuspending the lipid in *n*-decane after 15 min (Sigma-Aldrich). Bilayers were formed by the planar lipid bilayer technique. Bilayers were formed across a 200-μm-diameter aperture in the septum by painting lipid dispersion across the (lipid-pretreated) septum. In Ca^{2+}-permeability experiments, the *cis*- and *trans*-chambers were filled with 0.5 mL 10 mM MES/*bis* Tris propane (BTP), 1 mM $CaCl_2$, pH 6.0, 2 mL 10 mM MES/BTP, and 200 mM $CaCl_2$, pH 6.0. In K^+-permeability experiments, the *cis*-chamber comprised 200 mM KCl and 10 mM MES/BTP, pH 6.0, and the *trans*-comprised 50 mM KCl and 10 mM MES-/TP, pH 6.0. The *cis*-compartment was connected to the headstage of the Axopatch 200B amplifier (Axon Instruments), and the *trans*-compartment was connected to the signal ground using agar-salt bridges (3 M KCl and 1% [w/v] agar) and Ag/AgCl electrodes. Bilayer formation was monitored electronically by capacitance measurements with their final capacitance ranging from 150 to 200 pF and their resistance from 2 to 5 GΩ. Following stable bilayer formation, 3 μg of annexin protein was added to the *cis*-chamber. The bilayer was held at −150 mV (*cis*-negative) to aid protein insertion, and the *cis*-chamber was magnetically stirred intermittently. Experiments were performed at room temperature (20 to 24°C). Antagonists were added to the *trans*-chamber as indicated in Results. Filter and sample frequency were 1 and 5 kHz, respectively, and data analysis was performed with Clampfit software (version 8). Positive current deflections indicated movement of positive charge from the *cis*- to the *trans*-chamber, while negative current defections indicated the movement of positive charge from the *trans*- to the *cis*-chamber. Holding potentials were all corrected for (measured) liquid junctions. Liquid junctions were measured and corrected. Permeability ratios were calculated using the Goldman equation with the assumption at the reversal potential (E_{rev}), $I_X + I_Y + I_Z = 0$ where X, Y, and Z are different species of ions (Véry and Davies, 2000). Curve fitting of data was performed using SigmaPlot (SPSS Science).

Peroxidase Assay and Heme Analysis

Assay buffer (50 mM K-phosphate, pH 7.4) was used to dilute all solutions. All assays (final volume 100 μL) were performed at room temperature in the dark in a black 96-well plate (Greiner Bio-One) and comprised 50 μM Amplex Red (10-acetyl-3,7-dihydroxyphenoxazine; Invitrogen), 1 mM H_2O_2 (Sigma-Aldrich), and protein (ANN33/35 preparation or HRP Type VI; Sigma-Aldrich). Resorufin fluorescence was measured using a 560-nm excitation filter and a 590-nm emission filter in a FLUO-star plate-reader (BMG). Proteins heated for 10 min at 95°C were used as negative controls. Fluorescence values from identical assays without protein were subtracted from all data. To assay for heme content, absorption spectra were obtained using a Thermospectronic UV visible spectrophotometer. Samples were analyzed in 100-μL capacity UVettes (Eppendorf).

Phylogenetic Analysis

Amino acid sequence alignment was performed using ClustalW (default parameters; Larkin et al., 2007) and edited in JalView (http://www.jalview.org; Clamp et al., 2004). Prediction of secretion was performed using SecretomeP (www.cbs.dtu.dk/services/secretomeP; Bendtsen et al., 2004).

Accession Numbers

Sequence data from this article can be found in the Arabidopsis Genome Initiative or GenBank/EMBL/NCBI RefSeq data libraries under the following accession numbers: gb:CAA10210 (Ca ANN24), gb:AAC33305 (Gh ANN), gb:CAA66900 (Zm ANN33), gb:CAA66901 (Zm ANN35), gb:ABC59685 (Zm LOX1), gb:ABC59686 (Zm LOX2), gb:ABC59687 (Zm LOX4), gb:CAA00083 (*Armoracia rusticana* horseradish peroxidase; HRP), gb:CAA71759 (*Sporobolus stapfianus* hypothetical protein), RefSeq:NP_174810 (At1g35720, At ANN1), RefSeq:NP_201307 (At5g65020, At ANN2), RefSeq:NP_001145 (human annexin 5 Anx5), RefSeq:NP_005630 (human synaptotagmin I; Syn I), RefSeq:NP_796376 (human synaptotagmin II; Syn II), and RefSeq:NP_002730 (human protein kinase C isoform gamma; PKC γ).

Supplemental Data

The following materials are available in the online version of this article.

Supplemental Figure 1. Purification of ANN33/35 from Etiolated Maize Coleoptiles by Lipid Affinity.

Supplemental Figure 2. Analysis of the Maize 23-kD Protein and 19-kD Protein from *Sporobolus stapfianus*.

Supplemental Figure 3. Immunoprecipitation of Zm ANN33/35 Prevents Conductance Formation in Planar Lipid Bilayers.

ACKNOWLEDGMENTS

This work was supported by the Biotechnology and Biological Science Research Council, the Isaac Newton Trust, the Cambridge Overseas

Trusts, and the University of Cambridge Department of Plant Sciences Research Fund. We thank A.G. Smith's group for equipment access, L. Packman for assistance in protein identification, P.J. White for guidance on bilayers, and John Banfield for bilayer technical assistance. We thank Stephen Chivasa, Peter Hepler, and Joan Rigau for helpful discussions on protein localization and the referees, whose insight improved this work.

Received March 20, 2008; revised December 11, 2008; accepted February 2, 2009; published February 20, 2009.

REFERENCES

Ali, R., Lemtiri-Chlieh, F., Tsaltas, D., Leng, Q., von Bodman, S., and Berkowitz, G.A. (2007). Death don't have no mercy and neither does calcium: *Arabidopsis* Cyclic Nucleotide Gated Channel2 and innate immunity. Plant Cell **19:** 1081–1095.

Arispe, N., Rojas, E., Genge, B.R., Licia, N.Y.W., and Wuthier, R.E. (1996). Similarity in calcium channel activity of Annexin V and matrix vesicles in planar lipid bilayers. Biophys. J. **71:** 1764–1775.

Babbin, B.A., Lee, W.Y., Parkos, C.A., Winfree, L.M., Akylldiz, A., Perretti, M., and Nusrat, A. (2006). Annexin 1 regulates SKCO-15 cell invasion by signalling through formyl peptide receptors. J. Biol. Chem. **281:** 19588–19599.

Bassani, M., Neumann, P.M., and Gepstein, S. (2004). Differential expression profiles of growth-related genes in the elongation zone of maize primary roots. Plant Mol. Biol. **56:** 367–380.

Bayer, E.M., Bottrill, A.R., Walshaw, J., Vigouroux, M., Naldrett, M.J., Thomas, C.L., and Maule, A.J. (2006). *Arabidopsis* cell wall proteome defined using multidimensional protein identification technology. Proteomics **6:** 301–311.

Bendtsen, J.D., Jensen, L.J., Blom, N., von Heijne, G., and Brunak, S. (2004). Feature-based prediction of non-classical and leaderless protein secretion. Protein Eng. Des. Sel. **17:** 349–356.

Blackbourn, H.D., Barker, P.J., Huskisson, N.S., and Battey, N.H. (1992). Properties and partial protein-sequence of plant annexins. Plant Physiol. **99:** 864–871.

Blackbourn, H.D., and Battey, N.H. (1993). Annexin-mediated secretory vesicle aggregation in plants. Physiol. Plant. **89:** 27–32.

Blackbourn, H.D., Walker, J.H., and Battey, N.H. (1991). Calcium-dependent phospholipid-binding proteins in plants. Planta **184:** 67–73.

Blomstedt, C.K., Gianello, R.D., Gaff, R.D., Hamill, J.D., and Neale, A.D. (1998). Differential gene expression in desiccation-tolerant and desiccation-sensitive tissue of the resurrection grass, *Sporobolus stapfianus.* Aust. J. Plant Physiol. **25:** 937–946.

Bohn, M., Heinz, E., and Lüthje, S. (2001). Lipid composition and fluidity of plasma membranes isolated from corn (*Zea mays* L.) roots. Arch. Biochem. Biophys. **387:** 35–40.

Breton, G., Vazquez-Tello, A., Danyluk, J., and Sarhan, F. (2000). Two novel intrinsic annexins accumulate in wheat membranes in response to low temperature. Plant Cell Physiol. **41:** 177–184.

Burger, A., Voges, D., Demange, P., Ruiz Perez, C., Huber, R., and Berendes, R. (1994). Structural and electrophysiological analysis of Annexin V mutants. J. Mol. Biol. **237:** 479–499.

Büschenschütz, K., Marten, I., Becker, D., Philippar, K., Ache, P., and Hedrich, R. (2005). Differential expression of K^+ channels between guard cells and subsidiary cells within the maize stomatal complex. Planta **222:** 968–976.

Cantero, A., Barthakur, S., Bushart, T.J., Chou, S., Morgan, R.O., Fernandez, M.P., Clark, G.B., and Roux, S.J. (2006). Expression profiling of the *Arabidopsis* annexin gene family during germination, de-etiolation and abiotic stress. Plant Physiol. Biochem. **44:** 13–24.

Carletti, P., Masi, A., Spolaore, B., De Laureto, P.P., De Zorzi, M., Turetta, L., Ferretti, M., and Nardi, S. (2008). Protein expression changes in maize roots in response to humic substances. J. Chem. Ecol. **34:** 804–818.

Carroll, A.D., Moyen, C., Van Kesteren, P., Tooke, F., Battey, N.H., and Brownlee, C. (1998). Ca^{2+}, annexins, and GTP modulate exocytosis from maize root cap protoplasts. Plant Cell **10:** 1267–1276.

Chang, W.W.P., Huang, L., Shen, M., Webster, C., Burlingame, A.L., and Roberts, J.K.M. (2000). Patterns of protein synthesis and tolerance of anoxia in root tips of maize seedlings acclimated to a low-oxygen environment, and identification of proteins by mass spectrometry. Plant Physiol. **122:** 295–317.

Cho, K., Jang, S., Huon, T., Park, S., and Han, O. (2007). Biochemical characterization of the dual positional specific maize lipoxygenase and the dependence of lagging and initial burst phenomenon on pH, substrate and detergent during pre-steady state kinetics. J. Biochem. Mol. Biol. **40:** 100–106.

Clamp, M., Cuff, J., Searle, S.M., and Barton, G.J. (2004). The Jalview Java Alignment Editor. Bioinformatics **20:** 426–427.

Clark, G., Cantero-Garcia, A., Butterfield, T., Dauwalder, M., and Roux, S.J. (2005b). Secretion as a key component of gravitropic growth: Implications for annexin involvement in differential growth. Gravit. Space Biol. Bull. **18:** 113–114.

Clark, G.B., Lee, D.W., Dauwalder, M., and Roux, S.J. (2005a). Immunolocalization and histochemical evidence for the association of two different *Arabidopsis* annexins with secretion during early seedling growth and development. Planta **220:** 621–631.

Clark, G.B., Sessions, A., Eastburn, D.J., and Roux, S.J. (2001). Differential expression of members of the annexin multigene family in *Arabidopsis.* Plant Physiol. **126:** 1072–1084.

Clark, G.B., Turnwald, S., Tirlapur, U.K., Haas, C.J., von der Mark, K., Roux, S.J., and Scheuerlein, R. (1995). Polar distribution of annexin-like proteins during phytochrome-mediated initiation and growth of rhizoids in the ferns *Dryopteris* and *Anemia.* Planta **197:** 376–384.

Delmer, D.P., and Potikha, T.S. (1997). Structures and functions of annexins in plants. Cell. Mol. Life Sci. **53:** 546–553.

Demidchik, V., Bowen, H.C., Maathuis, F.J.M., Shabala, S.N., Tester, M.A., and Davies, J.M. (2002). *Arabididopsis thaliana* root nonselective cation channels mediate calcium uptake and are involved in growth. Plant J. **32:** 799–808.

Demidchik, V., and Maathuis, F.J.M. (2007). Physiological roles of nonselective cation channels in plants: from salt stress to signalling and development. New Phytol. **175:** 387–404.

Demidchik, V., Shabala, S.N., Coutts, K.B., Tester, M.A., and Davies, J.M. (2003). Free oxygen radicals regulate plasma membrane Ca^{2+} & K^+-permeable channels in plant root cells. J. Cell Sci. **116:** 81–88.

Diatloff, E., Roberts, M., Sanders, D., and Roberts, S.K. (2004). Characteristics of anion channels in the plasma membrane of Arabidopsis epidermal root cells and the identification of a citrate-permeable channel induced by phosphate starvation. Plant Physiol. **136:** 4136–4149.

Dodd, A.N., Kyed Jakobsen, M., Baker, A.J., Telzerow, A., Hou, S.-W., Laplaze, L., Barrot, L., Poethig, R.S., Haseloff, J.P., and Webb, A.A.R. (2006). Time of day modulation of Ca^{2+} signals in Arabidopsis. Plant J. **48:** 962–973.

Foreman, J., Demidchik, V., Bothwell, J.H.F., Mylona, P., Miedema, H., Torres, M.A., Linstead, P., Costa, S., Brownlee, C., Jones, J.D. G., Davies, J.M., and Dolan, L. (2003). Reactive oxygen species produced by NADPH oxidase regulate plant cell growth. Nature **422:** 442–446.

Gaymard, F., Pilot, G., Lacombe, B., Bouchez, D., Bruneau, D., Boucherez, J., Michaux-Ferrière, N., Thibaud, J.-B., and Sentenac, H. (1998). Identification and disruption of a plant Shaker-like outward channel involved in K^+ release into the xylem sap. Cell **94:** 647–655.

Gerke, V., and Moss, S.E. (2002). Annexins: From structure to function. Physiol. Rev. **82:** 331–371.

Gidrol, X., Sabelli, P.A., Fern, Y.S., and Kush, A.K. (1996). Annexin-like protein from *Arabidopsis thaliana* rescues Δ*oxyR* mutant of *Escherichia coli* from H_2O_2 stress. Proc. Natl. Acad. Sci. USA **93:** 11268–11273.

Golczak, M., Kicinska, A., Bandorowicz-Pikula, J., Buchet, R., Szewczyk, A., and Pikula, S. (2001). Acidic pH-induced folding of annexin VI is a prerequisite for its insertion into lipid bilayers and formation of ion channels by the protein molecules. FASEB J. **16:** 1083–1085.

Gorecka, K., Thouverey, C., Buchet, R., and Pikula, S. (2007). Potential role of annexin AnnAt1 from *Arabidopsis thaliana* in pH-mediated cellular response to environmental stimuli. Plant Cell Physiol. **48:** 792–803.

Gorecka, K.M., Konopka-Postupolska, D., Hennig, J., Buchet, R., and Pikula, S. (2005). Peroxidase activity of annexin 1 from *Arabidopsis thaliana.* Biochem. Biophys. Res. Commun. **336:** 868–875.

Hille, B. (1992). Ionic channels of excitable membranes. (Sinauer: Sunderland, MA) 2nd ed.

Hochholdinger, F., Woll, K., Guo, L., and Schnable, P.S. (2005). The accumulation of abundant soluble proteins changes early in the development of the primary roots of maize (*Zea mays* L.). Proteomics **5:** 4885–4893.

Hofmann, A., Delmer, D.B., and Wlodawer, A. (2003). The crystal structure of annexin Gh1 from *Gossypium hirsutum* reveals an unusual S_3 cluster. Eur. J. Biochem. **270:** 2557–2564.

Hofmann, A., Proust, J., Dorowski, A., Schantz, R., and Huber, R. (2000). Annexin 24 from *Capsicum annuum* X-ray structure and biochemical characterization. J. Biol. Chem. **275:** 8072–8082.

Hua, B.G., Mercier, R.W., Zielinski, R.F., and Berkowitz, G.A. (2003). Functional interaction of calmodulin with a plant cyclic nucleotide gated cation channel. Plant Physiol. Biochem. **41:** 945–954.

Isas, J.M., Patel, D.R., Jao, C., Jayasinghe, S., Cartailler, J.P., Haigler, H.T., and Langen, R. (2003). Global structural changes in annexin 12. The role of phospholipid, Ca^{2+}, and pH. J. Biol. Chem. **278:** 30227–30234.

Jami, S.K., Clark, G.B., Turlapati, S.W., Handley, C., Roux, S.J., and Kirti, P.B. (2008). Ectopic expression of an annexin from *Brassica juncea* confers tolerance to abiotic stress treatments in transgenic tobacco. Plant Physiol. Biochem. **46:** 1019–1030.

Jones, D.L., Blancaflor, E.B., Kochian, L.V., and Gilroy, S. (2006). Spatial coordination of aluminium uptake, production of reactive oxygen species, callose production and wall rigidification in maize roots. Plant Cell Environ. **29:** 1309–1319.

Ketchum, K.A., Shrier, A., and Poole, R.J. (1989). Characterization of potassium-dependent currents in protoplasts of corn suspension cells. Plant Physiol. **89:** 1184–1192.

Kim, Y.-C., Kim, S.-Y., Choi, D., Ryu, C.-M., and Park, J.M. (2008). Molecular characterization of a pepper C2 domain-containing SRC2 protein implicated in resistance against host and non-host pathogens and abiotic stresses. Planta **227:** 1169–1179.

Kim, Y.J., Kim, J.E., Lee, J.H., Lee, M.H., Jung, H.W., Bahk, Y.Y., Hwang, B.K., Hwang, I., and Kim, W.T. (2004). The *Vr-PLC3* gene encodes a putative plasma membrane-localized phosphoinositide-specific phospholipiase C whose expression is induced by abiotic stress in mung bean (*Vigna radiate* L.). FEBS Lett. **556:** 127–136.

Kourie, J.I., and Wood, H.B. (2000). Biophysical and molecular properties of annexin-formed channels. Prog. Biophys. Mol. Biol. **73:** 91–134.

Kukavica, B., Quartacci, M.F., Veljović-Jovanović, S., and Navari-Izzo, F. (2007). Lipid composition of pea (*Pisum sativum* L.) and maize (*Zea mays* L.) root plasma membrane and membrane-bound peroxidase and superoxide dismutase. Arch. Biol. Sci. **59:** 295–302.

Kwak, J.M., Nguyen, V., and Schroeder, J.I. (2006). The role of reactive oxygen species in hormonal responses. Plant Physiol. **141:** 323–329.

Kwon, H., Yokoyama, R., and Nishitani, K. (2005). A proteomic approach to apoplastic proteins involved in cell wall regeneration in protoplasts of *Arabidopsis* suspension-cultured cells. Plant Cell Physiol. **46:** 843–857.

Langen, R., Isas, J.M., Hubbell, W.L., and Haigler, H.T. (1998). A transmembrane form of annexin XII detected by site-directed spin labelling. Proc. Natl. Acad. Sci. USA **95:** 14060–14065.

Larkin, M.A., et al. (2007). Clustal W and Clustal X version 2.0. Bioinformatics **23:** 2947–2948.

Lee, S., Lee, E.J., Yang, E.J., Lee, J.E., Park, A.R., Song, W.H., and Park, O.K. (2004). Proteomic identification of annexins, calcium-dependent membrane binding protein that mediate osmotic stress and abscisic acid signal transduction in *Arabidopsis.* Plant Cell **16:** 1378–1391.

Leng, Q., Mercier, R.W., Hua, B.G., Fromm, H., and Berkowitz, G.A. (2002). Electrophysiological analysis of cloned cyclic nucleotide-gated ion channels. Plant Physiol. **128:** 400–408.

Liemann, S., Benz, J., Burger, A., Voges, D., Hofmann, A., Huber, R., and Göttig, P. (1996). Structural and functional characterisation of the voltage sensor in the ion channel human annexin V. J. Mol. Biol. **258:** 555–561.

Liszkay, A., van der Zalm, E., and Schopfer, P. (2004). Production of reactive oxygen intermediates ($O_2^{\cdot-}$, H_2O_2, and $^{\cdot}OH$) by maize roots and their role in wall loosening and elongation growth. Plant Physiol. **136:** 3114–3123.

Margoliash, E., and Frohwirt, N. (1959). Spectrum of horse-heart cytochrome C. Methods Enzymol. **71:** 570–572.

Markoff, A., Bogdanova, N., Knop, M., Rüffer, C., Kenis, H., Lux, P., Reutelingsperger, C., Todorov, V., Dworniczak, B., Horst, J., and Gerke, V. (2007). Annexin A5 interacts with Polycystin-1 and interferes with the Polycystin-1 stimulated recruitment of E-cadherin into adherens junctions. J. Mol. Biol. **369:** 954–966.

Marshall, J., Corzo, A., Leigh, R.A., and Sanders, D. (1994). Membrane potential-dependent calcium transport in right-side-out plasma membrane vesicles from *Zea mays* L. roots. Plant J. **5:** 683–694.

McAinsh, M.R., Clayton, H., Mansfield, T.A., and Hetherington, A.M. (1996). Changes in stomatal behaviour and guard cell cytosolic free calcium in response to oxidative stress. Plant Physiol. **111:** 1031–1042.

McClung, A.D., Carroll, A.D., and Battey, N.H. (1994). Identification and characterization of ATPase activity associated with maize (*Zea mays*) annexins. Biochem. J. **30:** 709–712.

Meyerhoff, O., Müller, K., Roelfsma, M.R.G., Latz, A., Lacombe, B., Hedrich, R., Dietrich, P., and Becker, D. (2005). *AtGLR3.4*, a glutamate receptor channel-like gene is sensitive to touch and cold. Planta **222:** 418–427.

Mittler, R., Vanderauwera, S., Gollery, M., and Van Breusegem, F. (2004). Reactive oxygen gene network of plants. Trends Plant Sci. **9:** 490–498.

Morgan, R.O., Martin-Almedina, S., Garcia, M., Jhoncon-Kooyip, J., and Fernandez, M. (2006). Deciphering function and mechanism of calcium-binding proteins from their evolutionary imprints. Biochim. Biophys. Acta **1763:** 1238–1249.

Morgan, R.O., Martin-Almedina, S., Iglesias, J.M., Gonzalez-Florez, M.I., and Fernandez, M.P. (2004). Evolutionary perspective on annexin calcium-binding domains. Biochim. Biophys. Acta **1742:** 133–140.

Mortimer, J.C. (2007). Plant Annexins: Calcium-Binding Peroxidases. PhD dissertation (Cambridge, UK: University of Cambridge).

Mortimer, J.C., Laohavisit, A., Macpherson, N., Webb, A., Brownlee, C., Battey, N.H., and Davies, J.M. (2008). Annexins: Multi-functional components of growth and adaptation. J. Exp. Bot. **59:** 533–544.

Moss, S.E., and Morgan, R.O. (2004). The annexins. Genome Biol. **5:** 219.

Nalefski, E.A., and Falke, J.J. (1996). The C2 domain calcium-binding motif: Structural and functional diversity. Protein Sci. **5:** 2375–2390.

Okamoto, T., Higuchi, K., Shinkawa, T., Isobe, T., Lörz, H., Koshiba, T., and Kranz, E. (2004). Identification of major proteins in maize egg cells. Plant Cell Physiol. **45:** 1406–1412.

Passardi, F., Cosio, C., Penel, C., and Dunand, C. (2005). Peroxidases have more functions than a Swiss army knife. Plant Cell Rep. **24:** 255–265.

Peiter, E., Maathuis, F.J.M., Mills, L.N., Knight, H., Pelloux, J., Hetherington, A.M., and Sanders, D. (2005). The vacuolar Ca^{2+}-activated channel TPC1 regulates germination and stomatal movement. Nature **434:** 404–408.

Philippar, K., Büschenschütz, K., Abshagen, M., Fuchs, I., Geiger, D., Lacombe, B., and Hedrich, R. (2003). The K^+ channel KZM1 mediates potassium uptake into the phloem and guard cells of the C_4 grass *Zea mays*. J. Biol. Chem. **278:** 16973–16981.

Pnueli, L., Liang, H., Rozenberg, M., and Mittler, R. (2003). Growth suppression, altered stomatal responses, and augmented induction of heat shock proteins in cytosolic ascorbate peroxidase (*Apx1*)-deficient *Arabidopsis* plants. Plant J. **34:** 187–203.

Porta, H., and Rocha-Sosa, M. (2002). Plant lipoxygenases. Physiological and molecular features. Plant Physiol. **130:** 12–21.

Roberts, S.K. (1998). Regulation of K^+ channels in maize roots by water stress and abscisic acid. Plant Physiol. **116:** 145–153.

Rouhier, N., and Jacquot, J.P. (2005). The plant multigenic family of thiol peroxidases. Free Radic. Biol. Med. **38:** 1413–1421.

Shang, Z.L., Ma, L.G., Zhang, H.L., He, R.R., Wang, X.C., Cui, S.J., and Sun, D.Y. (2005). Calcium influx into lily pollen grains through a hyperpolarization activated Ca^{2+}-permeable channel which can be regulated by extracellular CaM. Plant Cell Physiol. **46:** 598–608.

Shin, R., and Schachtman, D.P. (2004). Hydrogen peroxide mediates plant root cell response to nutrient deprivation. Proc. Natl. Acad. Sci. USA **101:** 8827–8832.

Su, Y.H., North, H., Grignon, C., Thibaud, J.-B., Sentenac, H., and Véry, A.-A. (2005). Regulation by external K^+ in a maize inward shaker channel targets transport activity in the high concentration range. Plant Cell **17:** 1532–1548.

Subbaiah, C.C., Kollipara, K.P., and Sachs, M.M. (2000). A Ca^{2+}-dependent cysteine protease is associated with anoxia-induced root tip death in maize. J. Exp. Bot. **51:** 721–730.

Tapken, D., and Hollmann, M. (2008). *Arabidopsis thaliana* glutamate receptor ion channel function demonstrated by ion pore transplantation. J. Mol. Biol. **383:** 36–48.

Thonat, C., Mathieu, C., Crevecoeur, M., Penel, C., Gaspar, T., and Boyer, N. (1997). Effects of a mechanical stimulation on localization of annexin-like proteins in *Bryonia dioica* internodes. Plant Physiol. **114:** 981–988.

Urquhart, W., Gunawardena, A.H.L.A.N., Moeder, W., Ali, R., Berkowitz, G.A., and Yoshioka, K. (2007). The chimeric cyclic nucleotide-gated ion channel ATCNGC11/12 constitutively induces programmed cell death in a Ca^{2+}-dependent manner. Plant Mol. Biol. **65:** 747–761.

Véry, A.-A., and Davies, J.M. (2000). Hyperpolarization-activated calcium channels at the tip of *Arabidopsis* root hairs. Proc. Natl. Acad. Sci. USA **97:** 9801–9806.

Wolf, T., Guinot, D.R., Hedrich, R., Dietrich, P., and Marten, I. (2005). Nucleotides and Mg^{2+} ions differentially regulate K^+ channels and non-selective cation channels present in cells forming the stomatal complex. Plant Cell Physiol. **46:** 1682–1689.

Yang, W.Q., Lai, Y., Li, M.-N., Xu, W.-Y., and Xue, Y.-B. (2008). A novel C2-domain phospholipids-binding protein, OsPB1, is required for pollen fertility in rice. Mol. Plant **1:** 770–785.

Zhang, W., Wang, C., Qin, C., Wood, T., Olafsdottir, G., Welti, R., and Wang, X. (2003). The oleate-stimulated phospholipiase D, PLDδ, and phosphatidic acid decrease H_2O_2-induced cell death in *Arabidopsis.* Plant Cell **15:** 2285–2295.

Zhou, M., Diwu, Z., Panchuk-Voloshina, N., and Haugland, R.P. (1997). A stable nonfluorescent derivative of resorufin for the fluorometric determination of trace hydrogen peroxide: Applications in detecting the activity of phagocyte NADPH oxidase and other oxidases. Anal. Biochem. **253:** 162–168.

Zhu, J., Chen, S., Alvarez, S., Asirvatham, V.S., Schachtman, D.P., Wu, Y., and Sharp, R.E. (2006). Cell wall proteome in the maize primary root elongation zone. I. Extraction and identification of water soluble and lightly ionically bound proteins. Plant Physiol. **140:** 311–325.

Zea mays Annexins Modulate Cytosolic Free Ca2+ and Generate a Ca2+-Permeable Conductance
Anuphon Laohavisit, Jennifer C. Mortimer, Vadim Demidchik, Katy M. Coxon, Matthew A. Stancombe, Neil Macpherson, Colin Brownlee, Andreas Hofmann, Alex A.R. Webb, Henk Miedema, Nicholas H. Battey and Julia M. Davies
PLANT CELL 2009;21;479-493; originally published online Feb 20, 2009;
DOI: 10.1105/tpc.108.059550

This information is current as of August 21, 2009

Supplemental Data	http://www.plantcell.org/cgi/content/full/tpc.108.059550/DC1
References	This article cites 89 articles, 39 of which you can access for free at: http://www.plantcell.org/cgi/content/full/21/2/479#BIBL
Permissions	https://www.copyright.com/ccc/openurl.do?sid=pd_hw1532298X&issn=1532298X&WT.mc_id=pd_hw1532298X
eTOCs	Sign up for eTOCs for *THE PLANT CELL* at: http://www.plantcell.org/subscriptions/etoc.shtml
CiteTrack Alerts	Sign up for CiteTrack Alerts for *Plant Cell* at: http://www.plantcell.org/cgi/alerts/ctmain
Subscription Information	Subscription information for *The Plant Cell* and *Plant Physiology* is available at: http://www.aspb.org/publications/subscriptions.cfm

© American Society of Plant Biologists

ADVANCING THE SCIENCE OF PLANT BIOLOGY